

**OPTIMIZATION OF GENERATION CAPACITY FOR A 100 PER CENT
RENEWABLE POWER SYSTEM IN BARBADOS**

by

Franco Perez

Bachelor of Science in Electrical Engineering, Santiago, Chile, 2014

A Thesis Submitted in Partial Fulfillment
of the Requirements for the Degree of

Masters of Science in Electrical Engineering

In the Graduate Academic Unit of Electrical and Computer Engineering

Supervisors: Liuchen Chang, Ph.D., Electrical and Computer Engineering
Eugene Hill, Ph.D., Electrical and Computer Engineering

Examining Board: Julian Meng, Ph.D., Electrical and Computer Engineering
Saleh Saleh, Ph.D., Electrical and Computer Engineering
Suprio Ray, Ph.D., Computer Science

This thesis is accepted by the
Dean of Graduate Studies

THE UNIVERSITY OF NEW BRUNSWICK

June 2019

©Franco Perez, 2019

ABSTRACT

This thesis explores an approach to determine the optimal renewable generation capacities to achieve a 100 per cent renewable penetration in the island of Barbados by year 2030. Five renewable resources are considered: onshore wind, utility-scale solar PV, rooftop solar PV, dispatchable generation, and storage. A two-stage temporal optimization based on the concept of residuals and costs is used and modelled with the optimization software LINGO to solve the problem under different scenarios.

The results show that by minimizing the residual variations it is possible to balance the need for backup generation and storage that will support the wind and solar integration. The more storage power capacity, the more wind and solar can be incorporated into the system. Different load demand forecasts or the presence of DSM and EV technologies significantly affect the outcome of the optimization. This work provides the boundaries and considerations needed to achieve the Barbados renewable target.

DEDICATION

I dedicate my dissertation work to my family in Chile, especially to my parents Oscar and Maria, who always encouraged me to pursue higher education, advance my career, and accomplish my dreams. They gave me the tools and emotional support to complete this enormous challenge in spite of all the obstacles on the way.

To Angela, for all her love and support, her patience, her advice and her continuous encouragement to go beyond the limits.

ACKNOWLEDGEMENTS

I would like to thank my supervisor and professor Dr. Eugene Hill, who guided and motivated me during the whole research process. His method of work, start with basic models and build it up in small steps, gave me the opportunity to learn and really understand complex concepts, which I used in my work. I also would like to express my admiration for his work, his knowledge of power systems and the passion and dedication he puts on his lectures to make them a “continuous learning process”, as he usually says.

I would like to thank Professor Dr. Liuchen Chang, who gave me the opportunity to come to the University of New Brunswick to study this master’s degree and who allowed me to be part of the fascinating NB Power and Emera Research Centre for Smart Grid Technologies.

Lastly, I would like to thank Angela Nunes, graduate student from the faculty of Forestry and Environmental Management, who helped me with optimization theory, made me understand the importance of system modelling, and introduced me to the software LINGO, which became the main tool used in my work.

Table of Contents

ABSTRACT	ii
DEDICATION	iii
ACKNOWLEDGEMENTS	iv
Table of Contents	v
List of Tables	vii
List of Figures	viii
List of Symbols and Abbreviations	xi
1 Introduction.....	1
1.1 Motivation	1
1.2 Objectives.....	3
1.3 Thesis organization.....	4
2 Literature Review.....	5
3 Load demand.....	9
3.1 Introduction	9
3.2 Load scenarios.....	11
4 Renewable Energy Sources.....	13
4.1 Introduction	13
4.2 Onshore Wind.....	13
4.3 Central Solar PV.....	16
4.4 Distributed Solar PV	19
4.5 Dispatchable Generation	22
4.6 Energy Storage	23
5 Methodology.....	26
5.1 Introduction	26
5.2 Residual Optimization of Wind and Solar	27
5.2.1 Method	27
5.2.2 Data	28
5.2.3 Mathematical Formulation.....	28
5.3 Cost Optimization of Wind and Solar	29
5.3.1 Method	29
5.3.2 Data	30
5.3.3 Mathematical Formulation.....	30
5.4 Cost Optimization of Dispatchable Generation and Storage	31
5.4.1 Method	31
5.4.2 Data	32
5.4.3 Mathematical Formulation.....	32
6 Residual Optimization of Wind and Solar	36

6.1	Introduction	36
6.2	Unconstrained Case	36
6.3	Generator-Constrained Case.....	39
6.4	Storage-Constrained Case	41
6.5	Effect of Distributed Solar	43
6.6	Effect of Load Demand	45
6.7	Selected Scenarios.....	49
7	Cost Optimization of Wind and Solar.....	54
7.1	Introduction	54
7.2	Results	54
8	Cost Optimization of Dispatchable Generation and Storage	57
8.1	Introduction	57
8.2	Technology costs	58
8.3	Capacity Results	58
8.4	Operational Results	63
9	Conclusion	67
9.1	Results and Discussion.....	67
9.2	Recommendations for Future Work.....	70
	References	72
	Appendix A.....	76
	Appendix B	77
	Appendix C	79
	Curriculum Vitae	

List of Tables

Table 3-1. Electric vehicle demand characteristics.....	10
Table 3-2. Possible load demand scenarios for the year 2030	11
Table 4-1. Descriptive statistics of onshore wind dataset.....	14
Table 4-2. Descriptive statistics for the utility-scale solar PV dataset.....	17
Table 4-3. Descriptive statistics for the distributed solar PV dataset	20
Table 4-4. Grid services provided by energy storage	24
Table 6-1. Results for the unconstrained case.....	38
Table 6-2. Results for generator-constrained case	40
Table 6-3. Results for storage-constrained case.....	42
Table 6-4. Power results for different levels of distributed solar PV	44
Table 6-5. Energy results for different levels of distributed solar PV	44
Table 6-6. Load demand scenarios	46
Table 6-7. Selected load demand scenarios	50

List of Figures

Figure 1.1. Example of residual energy when having wind and solar generation	2
Figure 3.1. Load demand forecasts for Barbados (2012-2036).	9
Figure 3.2. Energy efficiency measures used for DSM load forecast (2012-2036).....	10
Figure 3.3. Comparison of daily electric vehicles charging profiles	11
Figure 3.4. Variation of average load demand profiles with additional EV load	12
Figure 4.1. Barbados wind map and wind farm site selected by AWS Truepower	14
Figure 4.2. Monthly mean capacity factor for onshore wind	15
Figure 4.3. Hourly capacity factors for onshore wind in Barbados	15
Figure 4.4. Best and worst days of the year for onshore wind production	16
Figure 4.5. Barbados solar map and solar farm site selected by AWS Truepower	17
Figure 4.6. Monthly mean capacity factor for utility-scale PV	18
Figure 4.7. Hourly capacity factors for utility-scale solar PV	18
Figure 4.8. Best and worst days of the year for utility-scale solar PV production	19
Figure 4.9. Distributed PV sites and density [16].	20
Figure 4.10. Monthly mean capacity factor for distributed solar PV	21
Figure 4.11. Comparison between central and distributed PV production for a week	21
Figure 4.12. Historical sugarcane production quantity in Barbados	23
Figure 4.13. Energy and power capacity of storage technologies	24
Figure 5.1. Methodology flow chart	27
Figure 5.2. Block diagram of residual optimization model of wind and solar	29
Figure 5.3. Block diagram for cost optimization model of storage and generator	35

Figure 6.1. Three-dimensional plot of the unconstrained objective function	37
Figure 6.2. Graphical solution for unconstrained case.....	38
Figure 6.3. Graphical solution for the generator-constraint case	40
Figure 6.4. Effect of load demand on the optimal wind and solar power capacities	47
Figure 6.5. Effect of load demand on wind and annual solar energy generated	47
Figure 6.6. Effect of load demand on maximum excess and shortage power residual.....	48
Figure 6.7. Effect of load demand on wind and solar annual residual energy	49
Figure 6.8. Optimal solar power capacity versus storage power, for the three load demand scenarios.....	51
Figure 6.9. Optimal wind power capacity versus storage power, for the three load demand scenarios.....	51
Figure 6.10. Optimal VRE capacity versus storage power, for the three load demand scenarios.....	52
Figure 6.11. Annual generation excess and shortage versus storage power, for the three load demand scenarios	53
Figure 7.1. Three dimensional representation of objective function	54
Figure 7.2. Contour plot of the cost objective function solution space	55
Figure 7.3. Cost optimization results for different values of storage and renewable level	56
Figure 8.1. Optimization solver status	57
Figure 8.2. Optimal generator power capacity for different levels of storage power, load demand and curtailed energy level.....	59
Figure 8.3. Optimal storage energy capacity for different levels of storage power, load demand and curtailed energy level.....	61

Figure 8.4. Annual Dispatchable generation for different levels of storage power, load demand and curtailed energy level.....	62
Figure 8.5. 10% curtailed energy for different levels of storage power and load demand	63
Figure 8.6. Monthly energy residuals for example case scenario	64
Figure 8.7. Hourly power residuals for example case scenario	64
Figure 8.8. Optimal hourly generation power dispatch for example case scenario	65
Figure 8.9. Optimal hourly storage power discharge for example case scenario	65
Figure 8.10. Optimal hourly storage power charge for example case scenario	65
Figure 8.11. Optimal hourly storage state of charge for example case scenario	66

List of Symbols and Abbreviations

Symbols:

CC_G	= Capital cost of dispatchable generator in \$/MW
CC_S	= Capital cost of storage power capacity in \$/MW
CC_H	= Capital cost of storage energy capacity in \$/MWh
CO_G	= Operation cost of dispatchable generator in \$/MWh
CO_S	= Operation cost of storage in \$/MWh
C_{uMAX}	= Maximum curtailed energy allowed in a year in %
$C_u(t)$	= Hourly curtailed power in MW
C_W	= Total cost of wind in \$/MW
C_S	= Total cost of solar in \$/MW
E_{Cu}	= Annual energy curtailment in MWh
E_G	= Annual energy generated by dispatchable generation unit in MWh
E_L	= Annual energy demand in MWh
E_{S1}	= Annual energy generated by solar PV – central in MWh
E_{S2}	= Annual energy generated by solar PV – distributed in MWh
E_W	= Annual energy generated by onshore wind in MWh
$F_{S1}(t)$	= Hourly capacity factors for solar PV – central in per unit
$F_{S2}(t)$	= Hourly capacity factors for solar PV – distributed in per unit
$F_W(t)$	= Hourly capacity factors for onshore wind in per unit
G	= Optimal dispatchable generator power capacity in MW
$G(t)$	= Hourly generator power dispatch in MW
G_{max}	= Maximum dispatchable generator power capacity in MW
G_{min}	= Minimum dispatchable generator power capacity in MW
H	= Optimal storage energy capacity in MWh
$H(t)$	= Hourly storage energy state of charge in MWh
H_{max}	= Maximum storage energy capacity in MWh
H_{min}	= Minimum storage energy capacity in MWh
$L(t)$	= Hourly load demand in MW
$R_E(t)$	= Hourly residual power excess in MW
RPL	= Renewable penetration level in the system in %
t	= Hour of the year from 1 to 8760
$R_S(t)$	= Hourly residual power shortage in MW

S	= Optimal storage rated power capacity in MW
S_1	= Installed power capacity for solar PV – central in MW
S_2	= Installed power capacity for solar PV – distributed in MW
$S_C(t)$	= Hourly storage power charge in MW
$S_D(t)$	= Hourly storage power discharge in MW
S_{max}	= Maximum storage power capacity in MW
S_{min}	= Minimum storage power capacity in MW
W	= Installed power capacity for onshore wind in MW

Abbreviations:

BESS	Battery Energy Storage System
BLPC	Barbados Light & Power Company Limited
CAES	Compressed Air Energy Storage
DSM	Demand Side Management
EV	Electric Vehicle
GHG	Green House Gases
IRP	Integrated Resource Plan
PHES	Pumped Hydro Energy Storage
PV	Photovoltaic
SOC	State of Charge
VRE	Variable Renewable Energy
WECC	Western Electricity Coordinating Council

1 Introduction

The primary objective of this research work is to determine possible combinations of renewable generation capacity to integrate 100 per cent renewable energy sources in the Caribbean island of Barbados by year 2030. This chapter presents the motivation of this work, the main objectives, and the organization of the document.

1.1 Motivation

Barbados is a small eastern Caribbean island located in the Atlantic Ocean. It has a population of 284,644 people in a total area of 432 km^2 , which results in a densely populated country. In size, it is 34 km north-to-south and 23 km east-to-west. The capital city is Bridgetown in the south west, where 25% of the population lives.

In the electricity sector, Barbados load demand reached 1,024 GWh in 2012, with a peak load demand of 167.5 MW. The generation mix is composed mainly of thermal generation units that use imported heavy fuel oil (85%) and diesel and jet fuel (15%) [1].

Nowadays, due to a lack of local refining infrastructure, the island of Barbados imports 100% of its fossil fuels to run the existing thermal generation, and that makes the cost of generating electricity very high and vulnerable to global oil price fluctuations [1]. For example, from 2006 to 2015 Barbados was importing 11,654 barrels of oil per day to meet its energy needs [2].

To eliminate this problem, reduce Green House Gas (GHG) emissions that cause climate change, and secure affordable and secure energy supply in the long term, Barbados made the commitment to integrate 100 per cent renewable energy sources by year 2030 [2].

The transition to renewable energy will involve the integration of a large amount of Variable Renewable Energy (VRE), especially wind and solar. It will also require dispatchable generation and energy storage to support the integration of VRE [3].

If a large amount of wind and solar is installed in the power system, a new concept of residuals arise. The residuals are defined as the instantaneous differences between the variable renewable generation (wind and solar) and the load demand. Figure 1.1 shows a typical example of using wind and solar generation to supply the load demand in Barbados. It can be seen that there are hours of the day with a generation surplus or positive residuals (in green) and hours with generation shortage or negative residuals (in red).

The uncontrollable and intermittent nature of wind and solar cause uncontrollable and intermittent residuals in the system. These residuals require controllable generation and storage to support the integration of wind and solar sources. Dispatchable generation would cover the negative residuals and storage would store the positive ones.

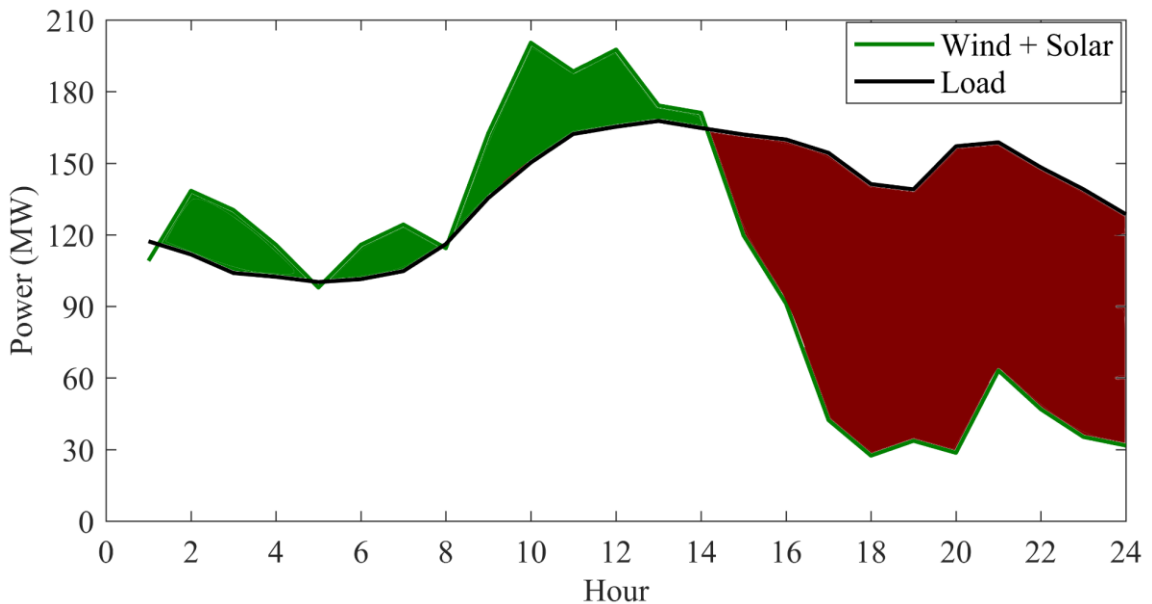


Figure 1.1. Example of residual energy when having wind and solar generation

Due to the uncontrollability and intermittency of the residuals, estimating the optimal generation mix among wind, solar, dispatchable, and storage generation capacities in an all-renewable power system becomes a challenge.

This research work combines the concept of residuals with optimization techniques to obtain optimal capacities for the renewable resources that will make possible the integration of 100 per cent renewable energy in Barbados.

1.2 Objectives

The main objectives of this research work are:

- To analyze the characteristics of the Barbados renewable generation resources and the forecast load demand profiles.
- To develop an optimization model using residuals to determine the optimal wind and solar capacities.
- To develop a cost optimization model to compare the results of wind and solar capacities obtained with those of the residuals method.
- To develop a cost optimization model to determine the dispatchable generation and storage capacities.
- To identify relationships among renewable generation resources.
- To determine the impact of using different load demand forecasts, Demand Side Management (DSM) technologies and Electric Vehicles (EV).
- To identify the benefits and limitations of the residuals-based optimization method.

1.3 Thesis organization

- Chapter 1 introduces the motivation for the problem, describes the Barbados system and sets out the objectives and organization of the document.
- Chapter 2 provides a description of the theory supporting the chosen methodology and also discusses research articles that are background for this research work.
- Chapter 3 analyzes and compares all the forecasted load demand profiles available for Barbados to prepare the input data for the optimization models.
- Chapter 4 analyzes the renewable resources available in Barbados to prepare the input data for the optimization models.
- Chapter 5 describes the methodology, assumptions, input data, and mathematical formulation of the optimization models used in this work.
- Chapter 6 shows the results for the wind and solar capacities obtained in the residual optimization model under different scenarios.
- Chapter 7 shows the results for the wind and solar capacities obtained in the cost optimization model under different scenarios.
- Chapter 8 shows the results for the dispatchable generation and storage capacities obtained in the cost optimization model under different scenarios.
- Chapter 9 states the main conclusions gathered from the findings of the optimization models and gives some recommendations for future work.

2 Literature Review

Optimization is used in several aspects of engineering such as design, operation, scheduling, finance, and many more. It helps in the decision-making process by selecting the best possible choice from a set of candidate alternatives. The solution method used for solving the optimization is an algorithm that depends on the form of the objective function, the form of constraints functions, and the number of variables and constraints [4].

The optimization of wind and solar capacities involves two decision variables in the problem with 8760 linear equations representing the power balance for every single hour of the year. This kind of problem is called “overdetermined linear system” because it has many more linear equations than unknown variables and each linear equation is of low quality. If the additional equations are neglected to solve the linear system, the results obtained will be of poor quality [5]. Overall, this type of problems has no exact solution. Instead, an approximate solution can be obtained by solving a minimization problem [6].

According to [5], overdetermined linear systems are formulated as,

$$A\hat{\mathbf{x}} \approx \mathbf{b} \quad (1)$$

Here A is an $m \times n$ matrix ($m > n$), with “ m ” representing the number of equations and “ n ” the number of decision variables of the problem. In our case of power balance equations $m = 8760$ and $n = 2$. The unknown decision variables are represented by an n -dimensional vector $\hat{\mathbf{x}}$, in our case the wind and solar capacities, and \mathbf{b} is a known measured vector, in our case the hourly load demand.

These type of problems can be solved by using the minimum l_1 , l_2 or the l_∞ norm approximate solution [5][7]. The l_1 norm finds the approximate solution of the problem by minimizing the sum of the residual magnitudes. The l_∞ norm minimizes the size of the

largest residual magnitude. The l_1 norm and the l_∞ norm are hard to solve in an efficient and robust manner, requiring nonlinear programming methods to find the solution [6][7]. The l_2 norm, also called the least squares method, is the simplest and most common approximate solution, and it can be solved by using a gradient method or quadratic programming. The least squares method finds an approximate solution by minimizing the sum of the squared residuals as shown in equation (2).

$$\min \sum_{i=1}^m \left(\sum_{j=1}^n A_{ij} \cdot X_j - b_i \right)^2 \quad (2)$$

By using square terms, the larger residuals have a more significant impact on the solution which is desirable for the wind and solar optimization because it avoids too much excess or shortage in hourly power [7].

Existing least squares algorithms (and software) are able to solve enormous problems, with hundreds of variables and constraints, and with high accuracy and reliability [4].

Several research works have used the concept of residuals to obtain the renewable generation capacities in a power system such as [8][9][10][11][12][13].

In the discussion paper [8] residual values were used to estimate the optimal capacities for Barbados by means of a simple simulation tool. The simulation tool computed the solar and wind power capacities necessary to meet the load demand every hour of the year. They used the solar radiation data from international databases and the wind speeds data from the island of Dominica which led to underestimating the wind resources. The final solution obtained was 195 MW solar, 200 MW wind, 3 GWh pumped hydro storage and 25 GWh biomass.

In [9] two models were developed to optimize renewable generation all over the western US. The first model uses the sum of the squared residuals to implicitly minimize the need for dispatchable generation and storage and obtaining the optimal values of wind and solar capacities. The model includes spatial optimization by considering 10,000 sites all over the western US, so different wind and solar profiles are necessary by location. The second model uses linear programming to minimize the operation of the backup generator and storage. The generator and storage capacities were not optimized because they were known variables in the model. Three main conclusions were reached in this study. The first one established that without storage, wind and photovoltaic (PV) generation could meet as much as 80% of the Western Electricity Coordinating Council (WECC) load only. Second, dispatchable generation can ensure that all loads are met and ramping requirements are not significant. Third, with a constrained storage significant amounts of wind and PV would have to be curtailed, especially in the spring when the wind blows and the load demand is low.

In [11] the variance of the residual demand is minimized to obtain the optimal capacities for run-of-river hydro, wind, and solar PV. The capacity factors for each one of the VRE and one year of load demand are used. No storage was considered, so a constraint in the model limits the maximum instantaneous share of renewable generation at every instant to limit the curtailment to zero, avoiding the need for storage and only minimizing the thermal generation production.

In [12] the objective is to minimize the standard deviation of the residual demand. Two renewables resources are considered in the model, onshore wind and solar PV. A spatial optimization is included by dividing the area into grid cells. No storage is considered.

In [13] the mix and spatial distribution of onshore wind, offshore wind, rooftop PV, and utility-scale PV capacities are optimized in Europe for the year 2050. The objective function minimizes the residuals. Europe is divided into 2000 grid cells to obtain the optimal results by location. The maximum penetration rate of wind and solar into the system reached 82% with a proportion of 74% wind, 26% solar PV, and 8% surplus.

In terms of optimization software tools, Matlab is used in [10], Microsoft Excel is used in [12], and GAMS/CPLEX is used in [14].

Most of the previous studies [9][13][11][12] consider the power system as a copperplate or single bus, neglecting the transmission lines.

To optimize the dispatchable generation and storage, an interesting approach is used in [14]. Linear programming is used in the optimization model, with several constraints that regulate the operation of the system and maintain the supply-demand balance. Two different types of models are tested and compared, a technical model called “load-matching optimization” and a cost minimization model that minimizes the cost of the system. The results are different for both models and the author states that cost optimization, has the disadvantage of being controlled by the price of the technologies.

Linear programming, unlike nonlinear programming, is able to find the global optimum and solve systems with hundreds of variables and thousands of constraints, with high accuracy and high reliability [4]. The problem must be formulated with an objective function and constraints as linear functions of the decision variables.

The literature review summarizes the references which are directly related to the optimization methodologies of the thesis. The remaining references are cited in context at appropriate points in the body of the document.

3 Load demand

3.1 Introduction

The load demand forecast for a 25-year planning horizon (2012-2036) was developed by Barbados Light and Power Company (BLPC) in its 2012 Integrated Resource Plan (IRP) [15]. Their estimation considered economic, demographic, and weather forecasts for Barbados for the next 25 years. Moreover, they included the following customer classes: residential, small commercial, large commercial, industrial, and streetlights.

To reflect uncertainty in the forecast profiles, they developed four levels of load demand forecast: low, medium, high, and Demand Side Management (DSM). Figure 3.1 shows the load forecast according to [15], starting from a 2012 load demand of 981 GWh/yr.

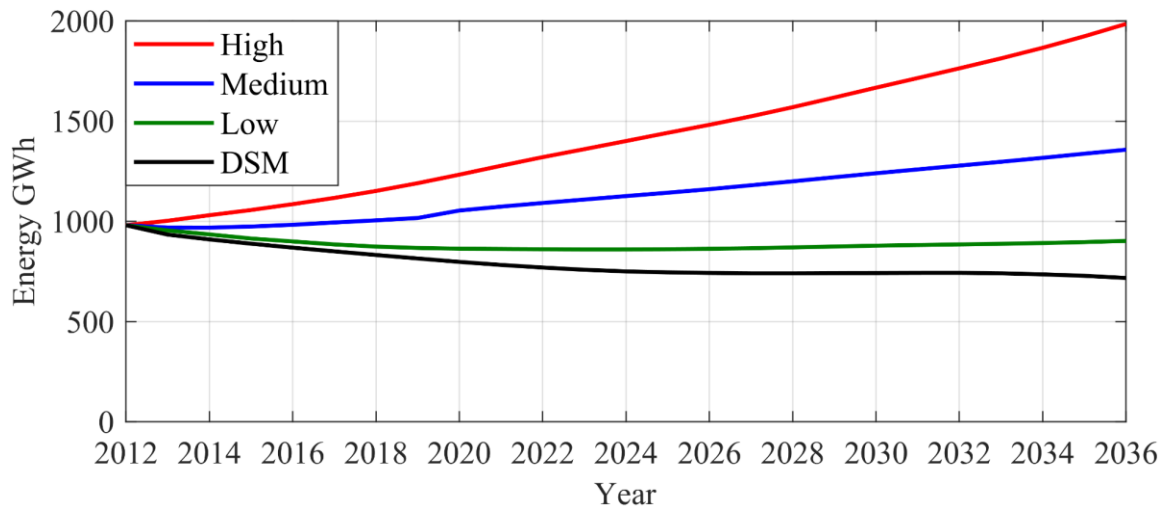


Figure 3.1. Load demand forecasts for Barbados (2012-2036).

The high load demand forecast was estimated with a 3.0% average growth rate per year, the medium load demand with a 1.2%, and the low load demand with -0.4%.

The load demand forecast with DSM technologies reduces the load demand significantly.

This DSM forecast includes the energy efficiency initiatives shown in Figure 3.2 [15].

Lighting	Compact fluorescent lamps (CFLs) T8 fluorescent lamps with occupancy sensor T5 high output fluorescent lamps Street lighting technologies (LED and solar LED)
Air Conditioning	Efficient window A/C systems Efficient split A/C systems
Refrigeration	Efficient residential refrigerators Efficient retail refrigerators
Mechanical	Premium efficiency motors Variable frequency drives Efficient chillers
Other	LCD computer monitors Power monitors

Figure 3.2. Energy efficiency measures used for DSM load forecast (2012-2036).

Another important technology that could affect the load demand in the Barbados forecast is the electric vehicles, which are penetrating the markets around the world in an exponential manner and are not considered in the IRP estimation.

The University of New Brunswick developed the load demand estimation for electric vehicles in Barbados, assuming a vehicle fleet of 16,000 in the year 2030. Two EV charging strategies are included in the estimation: home charging and work charging.

Table 3-1 shows the main characteristics of both EV profiles. Although the difference is negligible in the total annual numbers, the daily load patterns are different, and they have to be considered in the optimization model. Figure 3.3 compares both charging profiles on an average daily basis.

Table 3-1. Electric vehicle demand characteristics

Parameter	Unit	Home Charging	Work Charging
Annual Energy	(GWh/year)	290,352	291,815
Peak demand	(MW)	103.01	104.53
Average demand	(MW)	33.15	33.31
Lowest demand	(MW)	0.00	0.00
Annual load factor	%	32.18	32.87

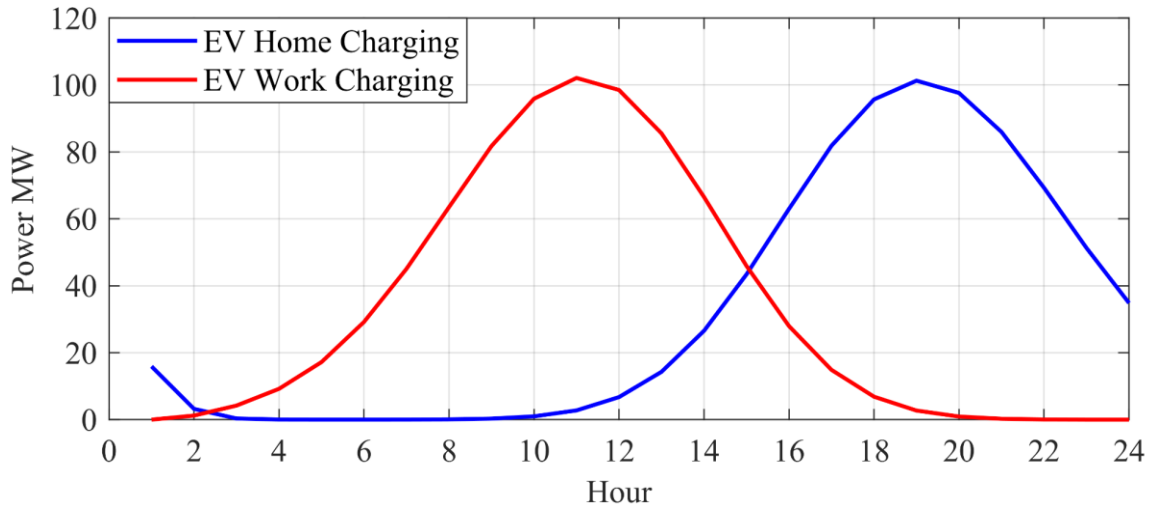


Figure 3.3. Comparison of daily electric vehicles charging profiles

3.2 Load scenarios

For the optimization model of this work, only the load demand profiles for the year 2030 are considered. There will be a total of 12 possible load demand profiles that can be used for the optimization models by combining low, medium, high and DSM load demand profiles with the EV home charging and EV work charging load profiles. Table 3-2 summarizes the load demand scenarios combinations.

Table 3-2. Possible load demand scenarios for the year 2030

Scenario	Load	EV Load	Energy	Peak	Average	Lowest	Load factor
			MWh/year	MW	MW	MW	%
1	Low	No EV	879,000	137.0	100.3	60.4	73.2
2	Medium		1,240,400	192.1	141.6	79.0	73.7
3	High		1,667,400	256.2	190.3	116.9	74.3
4	DSM		742,500	115.1	84.8	51.4	73.6
5	Low	Home Charging EV	1,169,352	232.4	133.5	60.4	57.4
6	Medium		1,530,752	280.4	174.7	79.5	62.3
7	High		1,957,752	347.2	223.5	116.9	64.4
8	DSM		1,032,852	211.6	117.9	51.4	55.7
9	Low	Work Charging EV	1,170,815	237.4	133.7	65.9	56.3
10	Medium		1,532,215	291.4	174.9	79.0	60.0
11	High		1,959,215	354.6	223.7	124.4	63.1
12	DSM		1,034,315	215.9	118.1	56.2	54.7

Figure 3.4, shows the forecasted load demand profiles on a daily average basis. The patterns have a similar shape. However, the energy and peak demand vary according to the category, from the lowest, the DSM load profile, to the high load demand.

The effect of adding the EV load demand profile to the system and the difference between home charging and work charging are also shown. Home charging increases the peak demand during the evenings when people arrive home and charge their vehicles. Work charging increases the peak demand during the daytime or office hours.

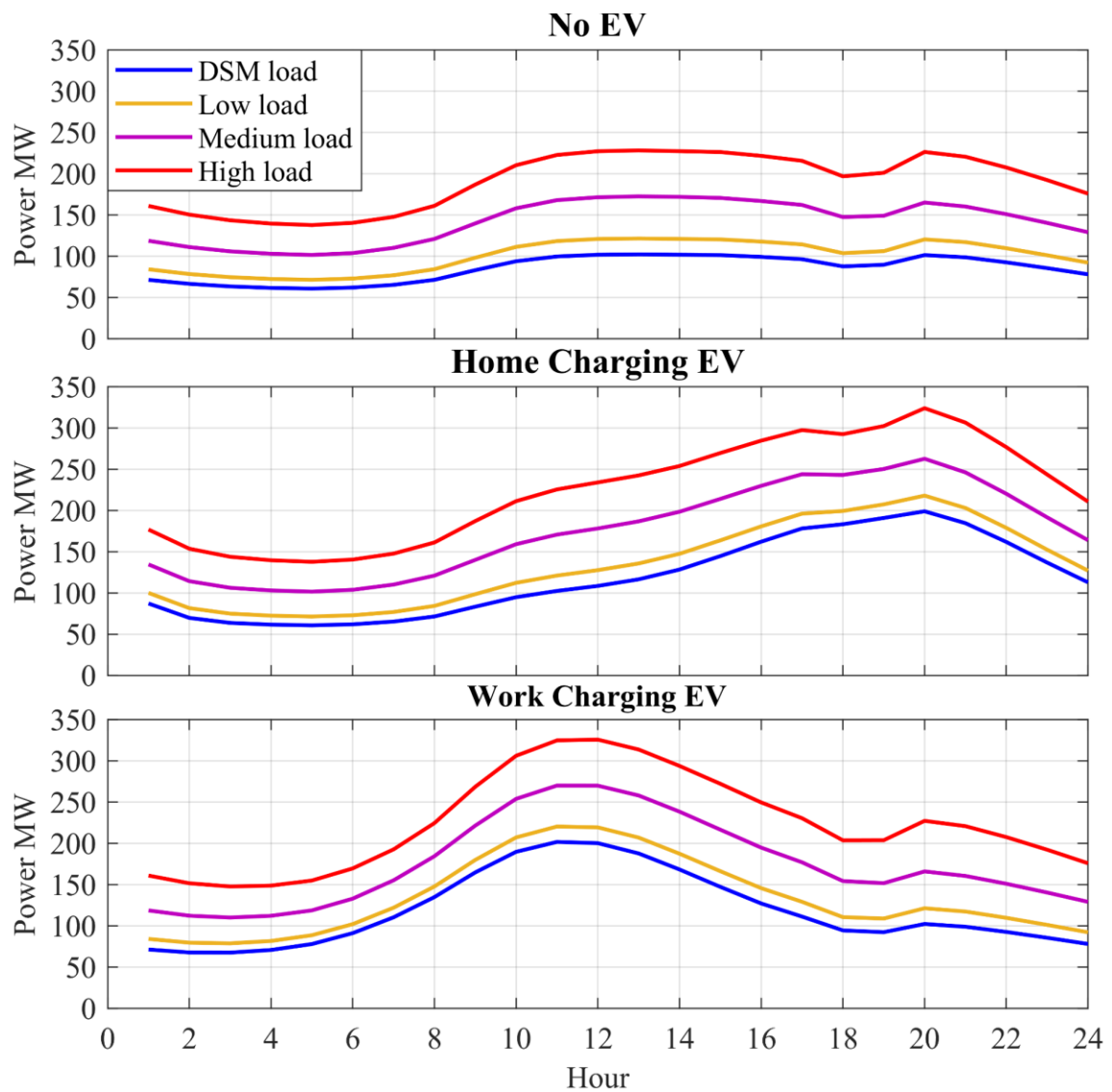


Figure 3.4. Variation of average load demand profiles with additional EV load

4 Renewable Energy Sources

4.1 Introduction

The following section describes the renewable energy sources considered for this research work. These are divided into four renewable generation categories: wind, solar, dispatchable generation, and energy storage.

Wind and solar are uncontrollable sources of energy and therefore they need to be estimated based on historical weather data on the island. The engineering company AWS Truepower developed the time series output data for these resources on the island of Barbados. They estimated the utility-scale solar PV, distributed or rooftop solar PV, and onshore wind data using historical weather data, rawinsonde (atmospheric) data, and land surface measurements [16]. These estimated profiles are analyzed in this section to get a better understanding of the resources.

In the category of dispatchable generation, no generation profile is necessary because the generation of these units is fully controllable. This section describes some alternatives of renewable dispatchable generation for the island of Barbados.

The last part of this section reviews some energy storage technologies that could be implemented on the island, but again without selecting any particular technology.

4.2 Onshore Wind

AWS Truepower assumed a wind farm located near the northern tip of the island on the windward side (east coast). This area has excellent wind potential according to Global Wind Data [17]; see Figure 4.1. The estimation of the onshore wind production data was developed using a mesoscale weather prediction model and the measurements from a 40m

tower nearby to adjust and validate the results. They modelled the wind plant at 50m hub height using the composite power curves of three types of wind turbines [16].

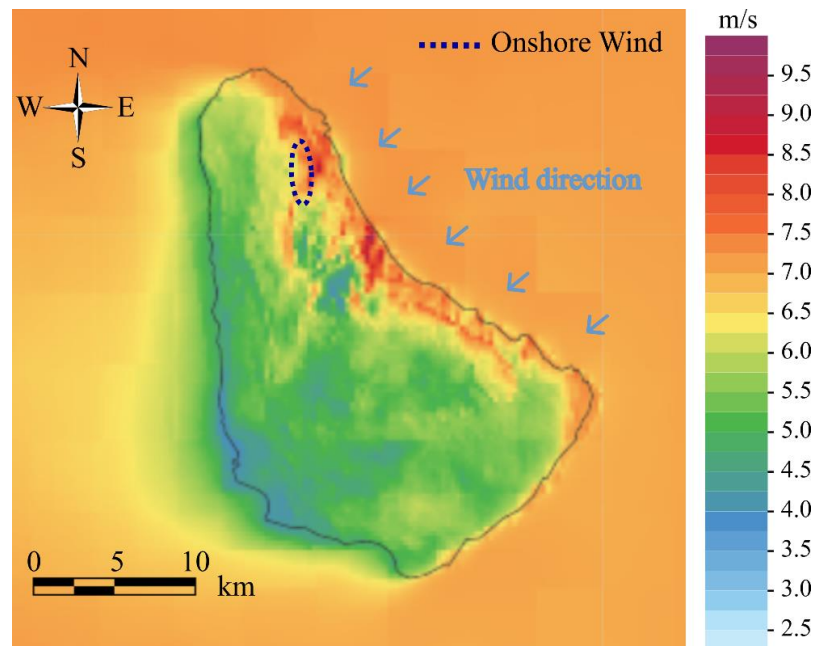


Figure 4.1. Barbados wind map and wind farm site selected by AWS Truepower

Source: Wind map obtained from “Global Wind Atlas 2.0”, <https://globalwindatlas.info>.

The wind production data are available in the form of normalized hourly capacity factors for a year. Table 4-1 shows a summary of the main parameters of this dataset. The summation of all the hourly capacity factors, with a value of 2784.5, implicitly represents the total energy that the onshore wind can produce in the year per MW of installed capacity. The onshore wind will generate on average 32% of its installed power capacity, and there will be hours with a maximum production of 81% and hours with zero output.

Table 4-1. Descriptive statistics of onshore wind dataset

Descriptive statistics	Value
Summation	2784.5
Mean	0.32
Maximum	0.81
Minimum	0.00
Standard deviation	0.20

Grouping the production data by month, it is possible to analyze the seasonal wind pattern of Barbados, as shown in Figure 4.2. Barbados only experiences two seasons, the “wet season” from June to November and the “dry season” from December to May [18]. The wind potential is low during the wet season, especially from August to October.

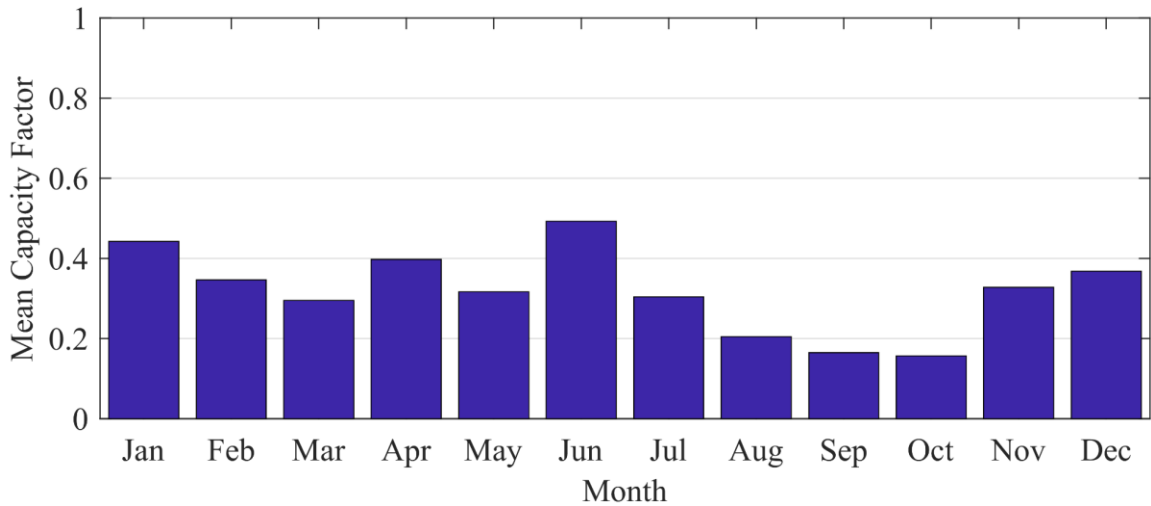


Figure 4.2. Monthly mean capacity factor for onshore wind

Figure 4.3, shows the hourly variation of the normalized wind power production. The intermittency and unpredictability of the wind resource cause daily, monthly, and seasonal differences.

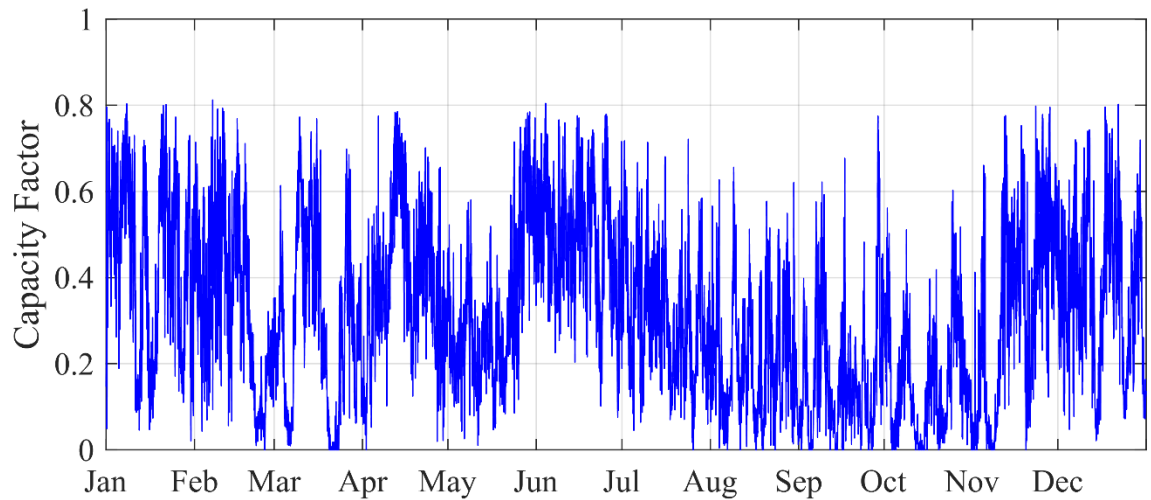


Figure 4.3. Hourly capacity factors for onshore wind in Barbados

Figure 4.4 illustrates the hourly wind capacity factors for two days of the year: These are with the lowest and highest average capacity factor. The worst day case has an average capacity factor of 0.35% which means that the wind farm will generate close to zero energy, requiring some other generation unit to cover the shortage. The best day has an average capacity factor of 70.52%. This big difference in power output confirms the need for operational flexibility in a power grid with wind generation.

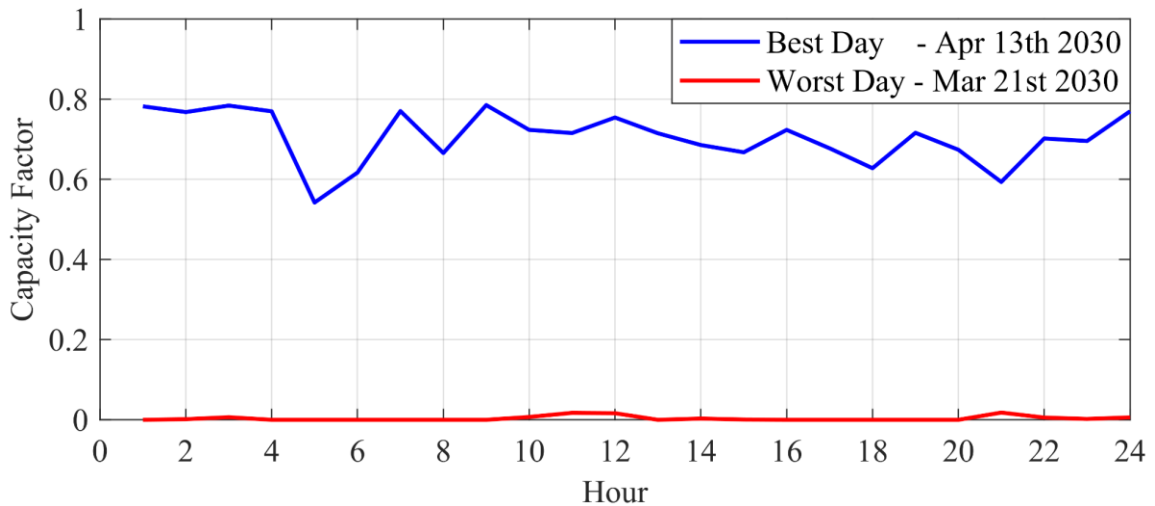


Figure 4.4. Best and worst days of the year for onshore wind production

4.3 Central Solar PV

AWS Truepower assumed a utility-scale solar PV farm near the northern part of the island and with a single-axis tracking system. The production data estimation was developed by combining a clear-sky model and a cloud model. The cloud coverage simulation captures the production ramp rates typical from solar farms [16]. Figure 4.5 shows the solar PV plant location and the solar potential for the island according to Global Solar Atlas Data [19]. The solar potential shown in the colour map is the long-term yearly averaged GHI (Global Horizontal Irradiation) potential expressed in kWh/m².

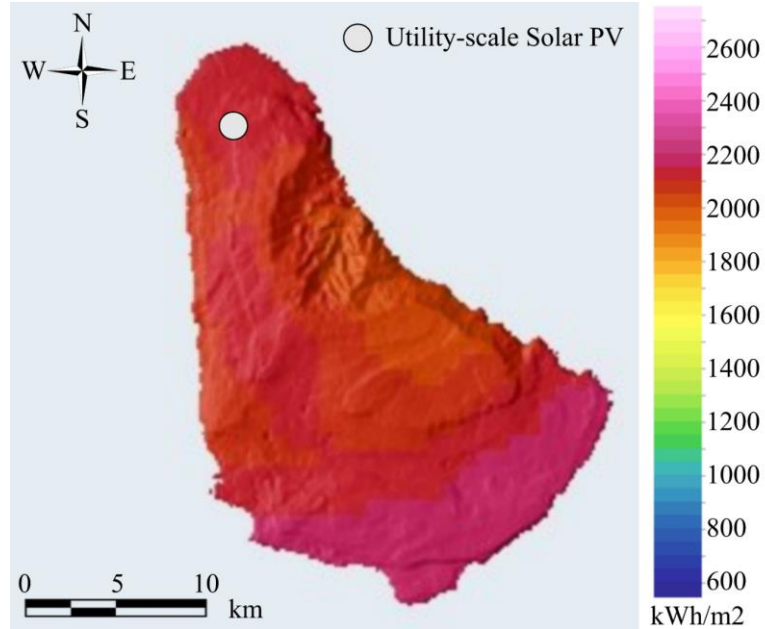


Figure 4.5. Barbados solar map and solar farm site selected by AWS Truepower

Source: Solar map adapted from Global Solar Atlas, owned by the World Bank Group and provided by Solaris. For additional information: <https://globalsolaratlas.info>

The solar PV production data is available in the form of normalized hourly capacity factors for a year. Table 4-2 shows a summary of the main parameters of this dataset. The summation of all the hourly capacity factors, with a value of 1615, implicitly represents the total energy per MW of installed capacity. The plant will generate on average 18% of its installed power capacity, and there will be hours with a maximum production of 87% and hours with zero production, during cloudy days and especially at night.

Table 4-2. Descriptive statistics for the utility-scale solar PV dataset

Descriptive statistics	Value
Summation	1615
Mean	0.18
Maximum	0.87
Minimum	0.00
Standard deviation	0.27

Grouping the production data by month, it is possible to analyze the seasonal solar pattern of Barbados, as shown in Figure 4.6. Barbados is sunny and has a warm climate all year round with an average temperature of 30°C during the day and more than 3,000 hours of sunshine in the year [20]. That is why the mean capacity factors are relatively uniform.

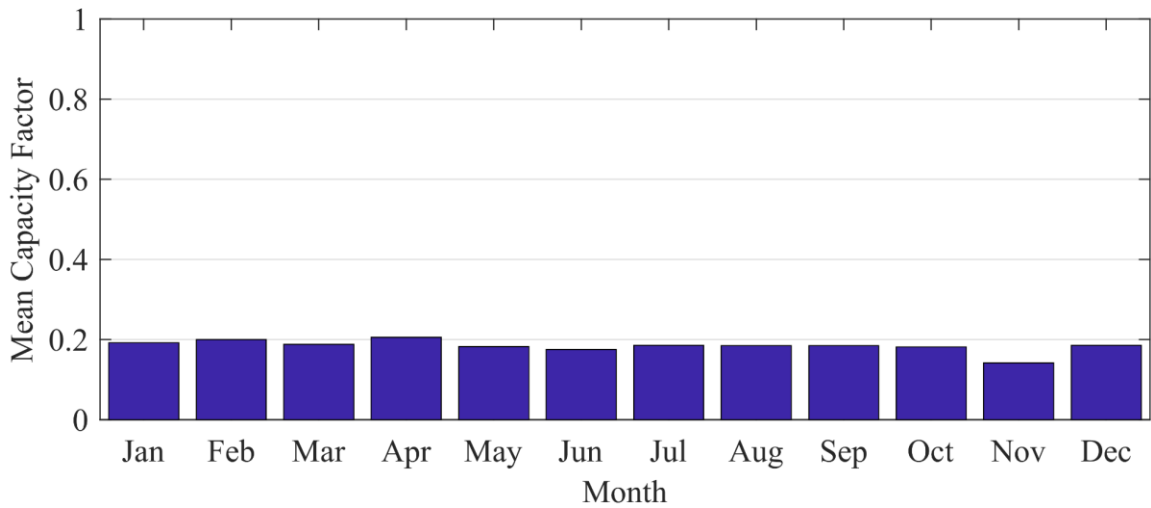


Figure 4.6. Monthly mean capacity factor for utility-scale PV

Figure 4.7 shows the hourly variation of the normalized central solar power production. It can be seen that the peak capacity factor varies from day to day.

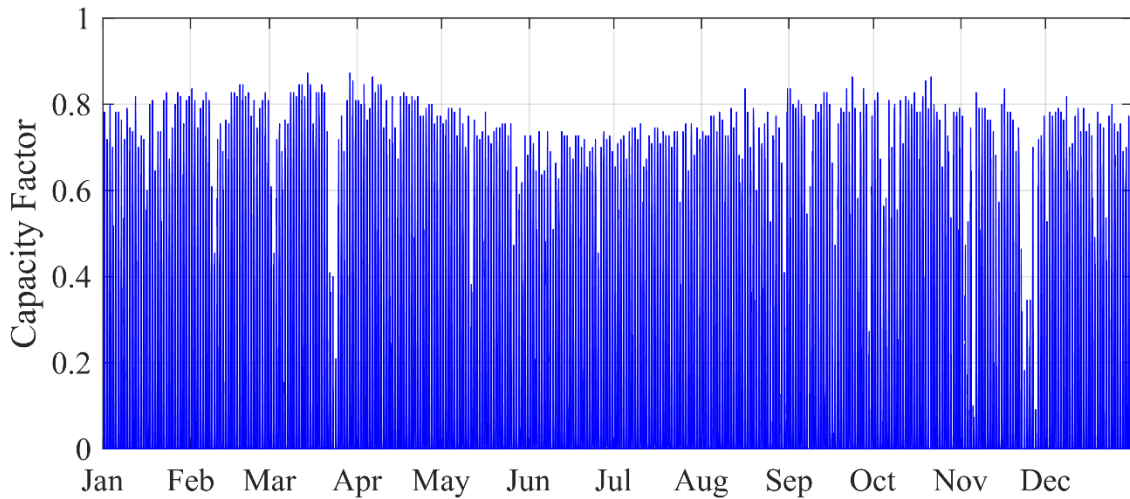


Figure 4.7. Hourly capacity factors for utility-scale solar PV

Figure 4.8 illustrates the central PV capacity factors for two days of the year. The days with the lowest and highest average capacity factor. The worst day case has an average capacity factor of 1.02% which means that the solar PV plant will generate close to zero power, requiring some other generation unit to cover the shortage. The best day has an average capacity factor of 24.68% with a peak value of 87.2% at midday.

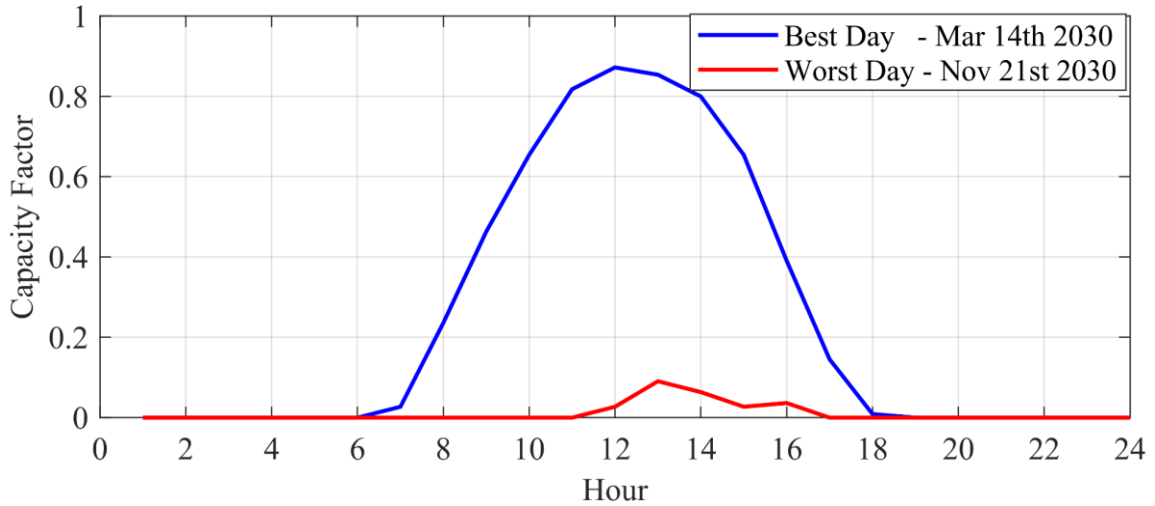


Figure 4.8. Best and worst days of the year for utility-scale solar PV production

4.4 Distributed Solar PV

According to [16], the distributed solar PV was assumed to be located mainly in urban areas, and they were aggregated and grouped by city and town. The distributed PV sites are shown in Figure 4.9. They were modelled with a fixed tilt axis at 30 degrees facing south [16]. The main advantage of rooftop solar installations over utility-scale solar PV farms is that they produce smoother power output during cloud coverage as the clouds only cover some locations at the same time and not the entire solar farm.

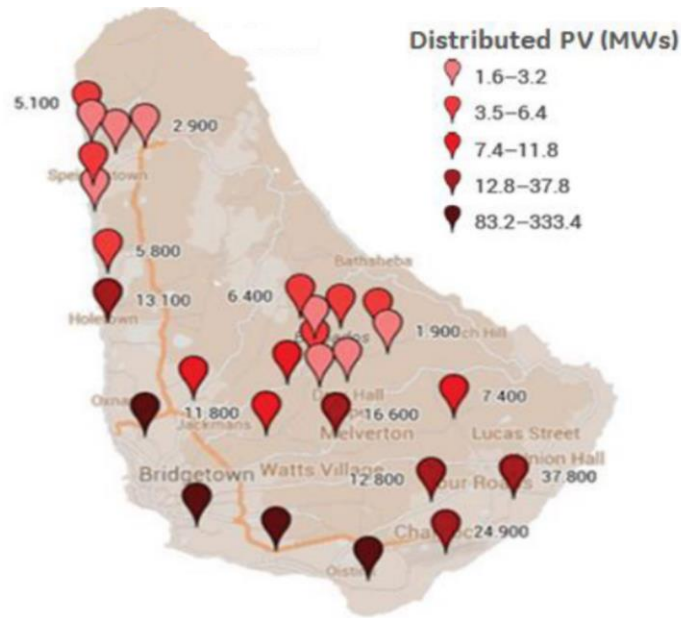


Figure 4.9. Distributed PV sites and density [16].

The solar PV production data is available in the form of normalized hourly capacity factors for a year. Table 4-3 shows a summary of the main parameters of this dataset. The summation of all the hourly capacity factors, with a value of 1909.4, implicitly represents the total energy that the distributed solar PV installations can produce in the year. They will generate on average 22% of its installed power capacity, and there will be hours with a maximum production of 93% and hours with zero output, during cloudy days and especially at night.

Table 4-3. Descriptive statistics for the distributed solar PV dataset

Descriptive statistics	Value
Summation	1909.4
Mean	0.22
Maximum	0.93
Minimum	0.00
Standard deviation	0.29

The monthly average production of distributed PV is slightly higher and with a similar pattern to the central solar PV farm because the sunlight resource is identical for both.

Figure 4.10 shows the monthly values.

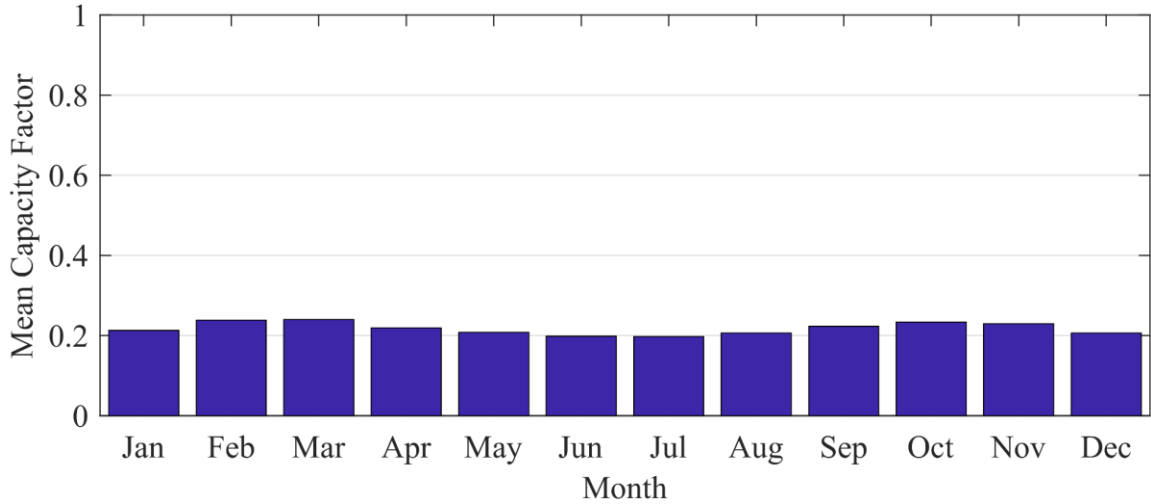


Figure 4.10. Monthly mean capacity factor for distributed solar PV

Figure 4.11 shows a comparison between central and distributed solar PV for a week in terms of hourly variations of power production. Distributed solar PV has fewer power output fluctuations and reaches higher capacity values in comparison to central PV. This is because moving clouds in the sky cannot cover all the locations at the same time.

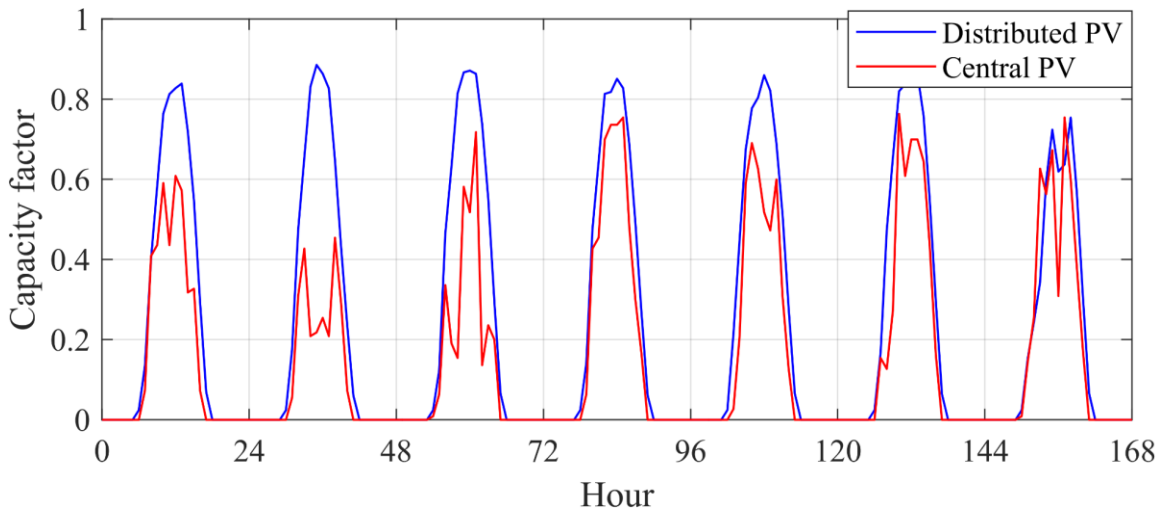


Figure 4.11. Comparison between central and distributed PV production for a week

4.5 Dispatchable Generation

Dispatchable resources can deliver power in a fully controllable manner to match the load demand at every instant. They become relevant in renewable power systems because they can be used to cover all the shortages in power supply due to the intermittencies from wind and solar resources, maintaining stability in the grid frequency and voltage [21].

Most of the dispatchable technologies are non-renewable such as coal, gas, diesel, and nuclear power plants [22]. However, there are some renewable generation technologies that are controllable such as geothermal, hydropower, and biomass [21].

Geothermal resources are usually near the boundaries of tectonic plates, use the natural underground hydrothermal energy, and can be detected by volcanoes, fumaroles, hot springs or geysers appearing on the earth's surface [23]. According to [15][24], the island of Barbados has zero potential for geothermal generation unlike some of the volcanic neighbouring islands.

The hydropower potential of the island is limited [24]. Hydropower energy depends on the availability of flowing water in rivers and the elevation difference. Barbados does not have any large rivers and is a relatively flat island [25].

Biomass generation plants transform wood, agricultural residues, and animal and human waste into electric power by methods such as direct combustion, gasification, pyrolysis, and anaerobic digestion [26]. For Barbados, the use of the bagasse from the sugar cane production and the transformation into liquid biofuels by the pyrolysis method is the most recommended path according to [8], because the liquid biofuel can be easily stored and be used in combustion engines which have low startup times and high ramp rates.

If Barbados does not generate enough biomass resources to feed their biomass power plants, it can be imported but at a higher price. According to the BLPC Integrated Resource Plan [15], local biomass fuel cost is estimated as 6.81-10.21 \$/MMBtu, and imported biomass is 29.80 – 38.03 \$/MMBtu.

The Barbados Cane Industry Corporation data shows that there is enough local sugar industry to sustain a 25MW biomass power plant [15]. However, it is important to highlight that the sugarcane production in Barbados has been decreasing steadily since 1968 as shown in Figure 4.12 [27].

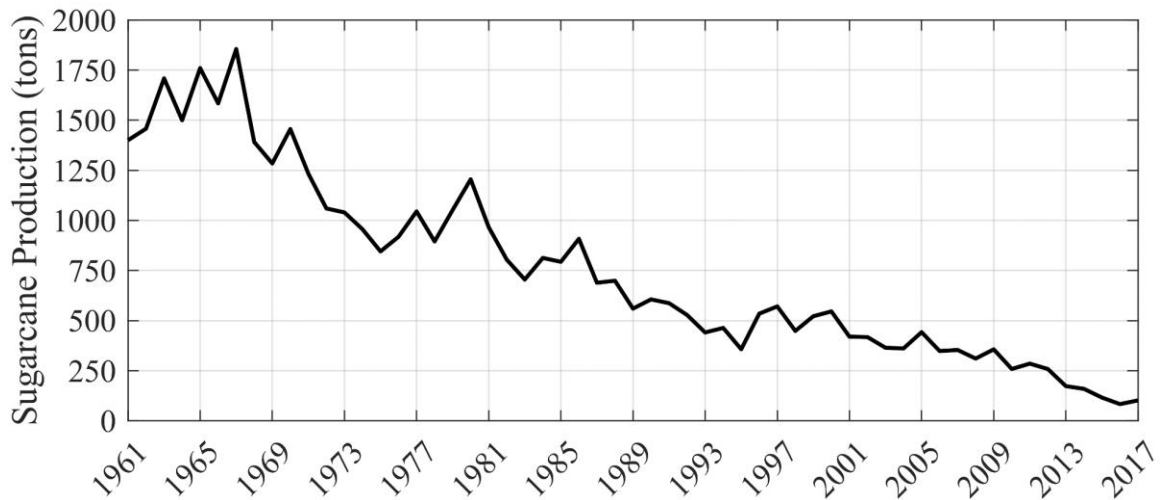


Figure 4.12. Historical sugarcane production quantity in Barbados

4.6 Energy Storage

Energy storage is fundamental for the integration of variable renewable generation because it can provide a wide range of grid services such as the ones shown in Table 4-4 [28].

Table 4-4. Grid services provided by energy storage

Bulk energy services	Electric energy time shift (arbitrage)
	Electric supply capacity
Ancillary services	Regulation, spinning, and non-spinning reserves
	Voltage support
	Black start
Transmission infrastructure services	Transmission upgrade deferral
	Transmission congestion relief
Distribution infrastructure services	Distribution upgrade deferral
	Voltage support
Customer energy management services	Power quality and reliability
	Retail electric energy time shift
	Demand charge management

For the purpose of this work, only bulk electric energy time shift and electric supply capacity grid services are considered to buffer the intermittencies of wind and solar generation and help maintain the supply-demand balance [21].

Energy storage technologies are defined by their power and energy capacities. For bulk energy-power applications there are only a few technologies that are feasible to use [29].

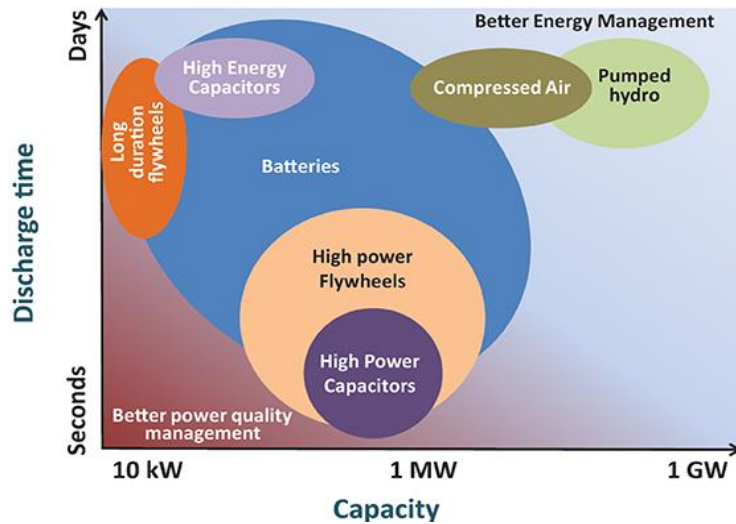


Figure 4.13. Energy and power capacity of storage technologies

According to Figure 4.13, the only technologies that can provide bulk energy shifting, long discharge times at high power capacity, for the power grid of Barbados are pumped hydro

storage (PHS), compressed air storage (CAES), and electrochemical batteries (BESS). CAES is an unfeasible solution because it requires large underground salt formations to form caverns and Barbados does not have them, as stated by [8]. Consequently, the only two technologies for storage in Barbados are PHS and BESS.

Pumped hydro storage is a large and mature technology, making up 96% of the total storage installed capacity in the world [30]. PHS stores energy in the form of water in a high-level reservoir. To store the energy, water is pumped from a lower reservoir to the high reservoir, and to discharge the energy, the water is released through turbines to produce electricity [31]. There are two types of PHS technologies: open-loop when the system is incorporated into natural rivers, lakes or reservoirs, and closed-loop when it is constructed independently of existing natural sources [32]. This last one makes up only 1% of existing PHS installations in the world [32].

According to [33], pumped hydro storage projects may be sized up to 4000MW and with a lifetime in the order of 50-60 years. For reference, an upper reservoir of one kilometer in diameter, 25 meters deep and a head of 200 meters would hold enough water to generate 10,000 MWh. In terms of costs of PHS, IRENA [28] estimates that the costs for PHS will remain stable until the year 2030, because the technology is already mature.

The second option, electrochemical energy storage technologies or BESS, are developing rapidly and they refer mostly to lithium-ion batteries, lead-acid batteries, sodium-sulfur batteries, and flow batteries. The Li-ion batteries are the most common for grid-side applications related to renewable integration, with 93% of the total installed capacity, followed by lead-acid batteries with the remaining 7% [30]. In comparison to pumped hydro storage, BESS are faster to implement because they do not require much civil work.

5 Methodology

5.1 Introduction

The optimization problem is solved in two stages. The first stage determines the capacity of the variable renewable generation, in this case, wind and solar PV resources. The second stage determines the capacity of the back-up dispatchable generation unit and the energy storage system. The first stage is solved by using a residual optimization model and a cost optimization model for comparison of results. The second stage is solved by using a cost optimization model only.

The models are developed in the modelling and optimization software LINGO version 18.0. LINGO is a comprehensive tool designed to build and solve linear, nonlinear, quadratic, quadratically constrained, stochastic, and integer optimization models. It provides its own modelling language and built-in solvers. LINDO SYSTEMS INC. is the company that owns the optimization software and offers a six-month renewable educational research license for the unrestricted capacity version [34].

A Microsoft Excel spreadsheet application was used as an interface with LINGO for handling and visualizing the input and output data. Figure 5.1 summarizes the procedure to be followed in this work.

The optimization models neglect the transmission lines and the siting of the renewable power plants because the Barbados power system is geographically small, and therefore, for the purpose of this study is considered a “copperplate” system where generation and load are connected in a single bus.

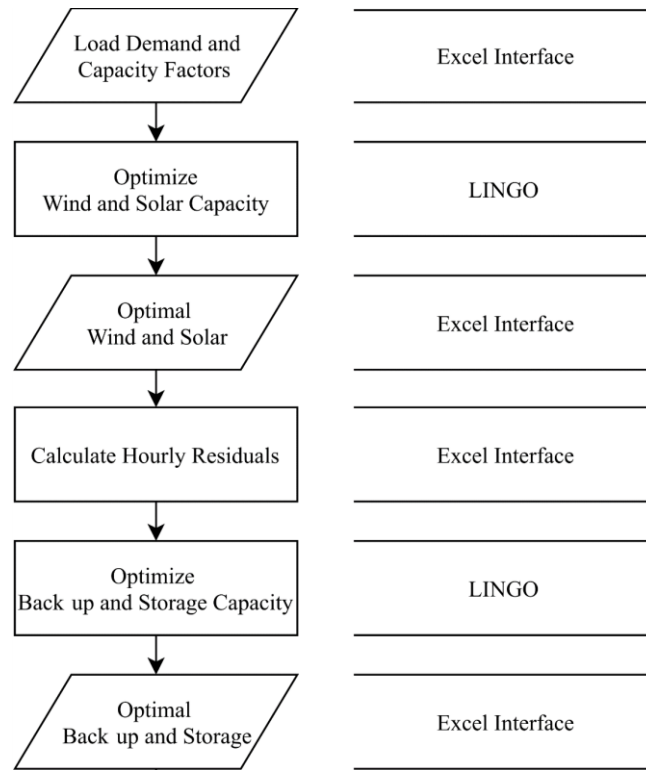


Figure 5.1. Methodology flow chart

5.2 Residual Optimization of Wind and Solar

5.2.1 Method

The residual optimization of VRES is done by using a linear least squares (LLSQ) method. This method minimizes the sum of the squares of the residuals which correspond to the residual demand values – the difference between the variable renewable generation (VRES) and the load demand – for every single hour. When minimizing the residual values, the model indirectly minimizes the back-up dispatchable generation and the storage required to cover the hourly load mismatches.

This first model does not consider costs in the objective function which makes the results independent of technology costs [6].

5.2.2 Data

The input data correspond to the hourly load demand and the normalized hourly capacity factors for all the VRES resources to be included in the optimization.

In the case of the load demand, there are different forecasts such as low, medium, and high load demand scenarios for the year 2030. There are also datasets including DSM and electric vehicle demand. Therefore, a sensitivity analysis can be carried out by using the different load demand datasets.

The normalized hourly capacity factors, from 0 to 1, are available for central solar PV, distributed PV and onshore wind.

5.2.3 Mathematical Formulation

The objective function (3) minimizes the sum of the squares of the hourly residuals for one year with an hourly resolution where the terms of the equations are defined in Figure 5.2.

Objective function:

$$\min f(W, S_1, S_2) = \sum_{t=1}^{8760} (W \cdot F_W(t) + S_1 \cdot F_{S1}(t) + S_2 \cdot F_{S2}(t) - L(t))^2 \quad (3)$$

Subject to:

Storage power constraint:

$$W \cdot F_W(t) + S_1 \cdot F_{S1}(t) + S_2 \cdot F_{S2}(t) - L(t) \leq S \quad \forall t \quad (4)$$

The constraint (4) limits the maximum excess power residual for every time interval to the desired value of storage that can store that power. This constraint allows storing any or all the excesses of VRE generation in the storage system, avoiding curtailment with the latter.

In the optimization, several values of storage power capacity are input.

Figure 5.2, shows a block diagram representation of this residual optimization model, including the outputs that can be computed with the results.

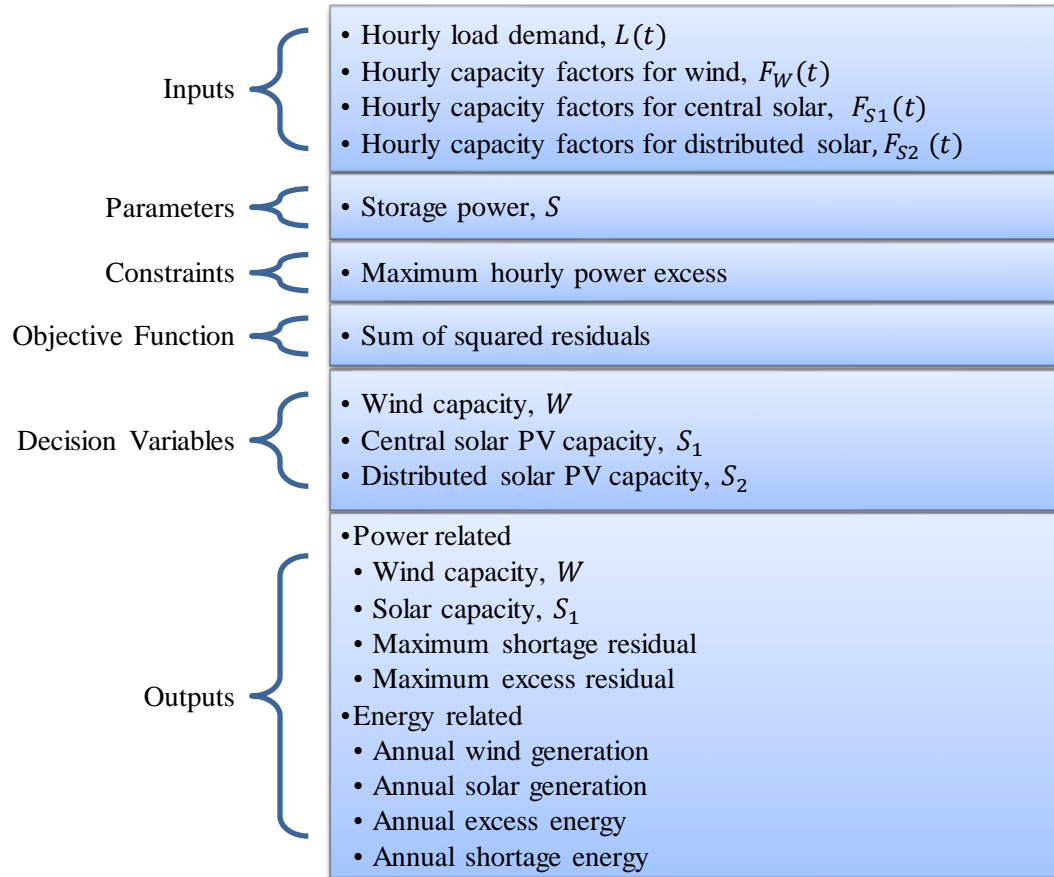


Figure 5.2. Block diagram of residual optimization model of wind and solar

5.3 Cost Optimization of Wind and Solar

5.3.1 Method

The cost optimization of wind and solar is modeled as a linear programming problem. The objective function minimizes the total cost of the system and the constraints enforce the maximum storage capacity limit and the desired renewable penetration level.

5.3.2 Data

The fixed input data correspond to the hourly load demand and the normalized hourly capacity factors for the wind and solar resources.

In the case of the load demand, there are different forecasts such as low, medium, and high load demand scenarios for the year 2030. There are also datasets including DSM and electric vehicle demand. Therefore, a sensitivity analysis can be carried out by using the different load demand datasets.

Apart from fixed input data, it is necessary to input the desired renewable penetration level in % and the maximum storage power capacity of the system. The penetration level represents the percentage of load energy that will be covered by the wind and solar annual generation. The maximum storage power in MW limits the maximum generation surplus allowed in the system. The total costs for wind and solar technologies are also required.

5.3.3 Mathematical Formulation

The objective function (5) minimizes the capital cost of the wind and solar generation mix where the terms are defined immediately below the equations.

Objective function:

$$\min f = C_S \cdot S_1 + C_W \cdot W \quad (5)$$

Subject to:

Storage power constraint:

$$W \cdot F_W(t) + S_1 \cdot F_{S1}(t) - L(t) \leq S \quad \forall t \quad (6)$$

Energy penetration constraint:

$$\sum_{t=1}^{8760} (W \cdot F_W(t) + S_1 \cdot F_{S1}(t)) \geq RPL \cdot E_L \quad (7)$$

Where

C_W	= Total cost of wind in \$/MW
C_S	= Total cost of solar in \$/MW
E_L	= Annual energy demand in MWh
$F_{S1}(t)$	= Hourly capacity factors for solar PV – central in per unit
$F_W(t)$	= Hourly capacity factors for onshore wind in per unit
$L(t)$	= Hourly load demand in MW
RPL	= Renewable penetration level in the system in %
S	= Optimal storage rated power capacity in MW
S_1	= Installed power capacity for solar PV – central in MW
W	= Installed power capacity for onshore wind in MW

The constraint (6) limits the maximum excess power residual for every time interval to the desired value of storage that can store that power. This constraint allows storing all the excesses of VRE generation in the storage system, avoiding curtailment. The optimization is run for several values of storage power capacity.

The constraint (7) forces the system to have enough wind and solar capacities to cover the desired percentage of the annual load demand. The variable RPL represents the renewable penetration level.

5.4 Cost Optimization of Dispatchable Generation and Storage

5.4.1 Method

This model optimizes the energy capability of the storage and the back-up dispatchable generation by minimizing the cost of the system. The resultant capacities will allow covering the shortages and excesses in the residual load hour by hour. The problem is modelled with linear programming employing five terms in the objective function.

The constraints regulate the operation between the dispatchable unit and the storage to cover the residual load values at every time interval.

5.4.2 Data

The main input datasets are the hourly power shortages and excesses in the residual load demand after computing the optimal wind and solar capacities from the first model. The excesses are either stored in the storage unit or curtailed. The shortages must be supplied by the dispatchable unit or the storage discharge.

The capital and operational costs for the dispatchable generator and storage are also required.

5.4.3 Mathematical Formulation

The objective function (8) minimizes the cost of the system by optimizing the power capacity of the dispatchable generator, the energy capability of the storage, and the annual operation of these two units to supply the residual load at all times.

The constraints regulate the hourly operation between the storage and dispatchable unit, and their maximum power and energy capacities. Figure 5.3, shows a block diagram representation of this cost optimization model and includes definition of the terms.

Objective function:

$$\min f = CC_G \cdot G + CC_H \cdot H + CO_G \cdot \sum_{t=1}^{8760} G(t) + CO_S \cdot \sum_{t=1}^{8760} S_D(t) + CO_S \cdot \sum_{t=1}^{8760} S_C(t) \quad (8)$$

Subject to constraints:

Energy balance:

$$G(t) + S_D(t) - S_C(t) - C_u(t) - R_S(t) + R_E(t) = 0 \quad \forall t \quad (9)$$

Dispatchable generator annual energy:

$$\sum_{t=1}^{8760} G(t) \geq \sum_{t=1}^{8760} (R_S(t) - R_E(t) + C_u(t)) \quad (10)$$

Dispatchable generator capacity limits:

$$G_{min} \leq G(t) \leq G \quad \forall t \quad (11)$$

$$G_{min} \leq G \leq G_{max} \quad (12)$$

$$G_{min} = 0 \text{ MW} \quad (13)$$

$$G_{max} = 400 \text{ MW} \quad (14)$$

Curtailment:

$$C_u(t) \geq 0 \quad \forall t \quad (15)$$

$$C_u(t) \leq S \quad \forall t \quad (16)$$

$$\sum_{t=1}^{8760} C_u(t) = C_{uMAX} \cdot \sum_{t=1}^{8760} (R_E(t)) \quad (17)$$

Storage state of charge:

$$H(t) = H(t-1) + S_C(t) - S_D(t) \quad \forall t \geq 2 \quad (18)$$

$$H(1) = 0.5 \cdot H + S_C(1) - S_D(1) \quad (19)$$

Storage energy capacity limits:

$$H_{min} \leq H(t) \leq H \quad \forall t \quad (20)$$

$$H_{min} \leq H \leq H_{max} \quad (21)$$

$$H_{min} = 0 \text{ MWh} \quad (22)$$

$$H_{max} = 40,000 \text{ MWh} \quad (23)$$

Storage power charge and discharge limits:

$$0 \leq S_C(t) \leq S \quad \forall t \quad (24)$$

$$0 \leq S_D(t) \leq S \quad \forall t \quad (25)$$

$$S_D(t) - R_S(t) \leq 0 \quad \forall t \quad (26)$$

Storage annual charging energy:

$$\sum_{t=1}^{8760} S_C(t) \geq \sum_{t=1}^{8760} R_E(t) - \sum_{t=1}^{8760} C_u(t) \quad (27)$$

Storage annual discharging energy:

$$\sum_{t=1}^{8760} S_D(t) \geq \sum_{t=1}^{8760} R_E(t) - \sum_{t=1}^{8760} C_u(t) \quad (28)$$

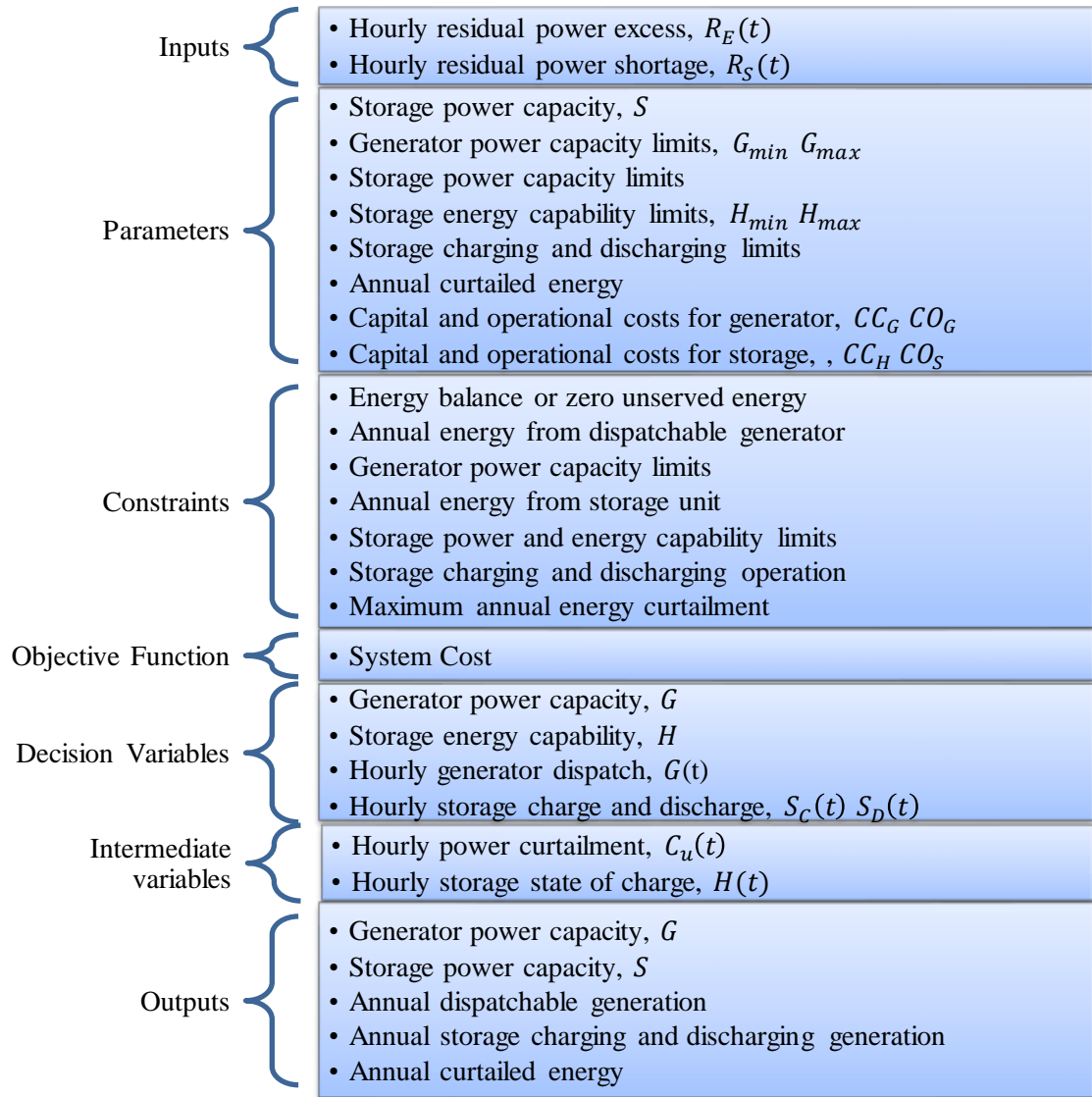


Figure 5.3. Block diagram for cost optimization model of storage and generator

6 Residual Optimization of Wind and Solar

6.1 Introduction

In this section, we present results from a series of cases that were run in the residual optimization model, starting from the simplest unconstrained model and adding complexity in small steps. The first cases only consider two decision variables: onshore wind and utility-scale solar PV.

The unconstrained model does not include any constraints, and it is used to show the properties of the model. The second case includes one annual energy constraint that forces the system to install enough wind and solar to supply the entire annual load demand. The third case includes a different constraint that limits the maximum excess power residual. The fourth case evaluates the effect of including distributed solar PV as a new decision variable in the problem and the last case assesses the impact of using different load demand profiles in the optimization.

A refined final model is selected considering only relevant parameters and with the load demand profiles that can give extreme values in the solution, taking into consideration that the other scenarios should be covered by these boundaries.

6.2 Unconstrained Case

The formulation does not include any constraint in this case, and the objective is to find the optimal wind and solar capacities that will minimize the residuals and indirectly minimize the values of both storage and dispatchable generation.

The objective function to be minimized is:

$$f(W, S_1) = \sum_{t=1}^{8760} (F_W(t) \cdot W + F_{S_1}(t) \cdot S_1 - L(t))^2$$

The expression above represents the objective function to be minimized to obtain the optimal wind and solar capacities. For this case, the medium load demand was used. Figure 6.1 shows the plot developed in Matlab for this function. The function is clearly convex so it has a global minimum which is the optimal point for the wind and solar capacities.

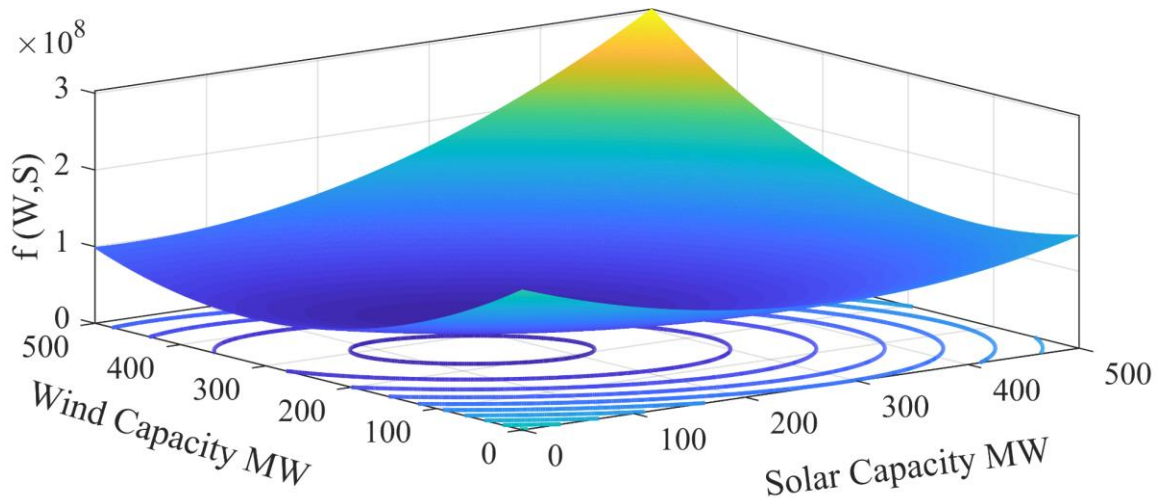


Figure 6.1. Three-dimensional plot of the unconstrained objective function

Figure 6.2 shows the contour graph that represents the three-dimensional surface shown previously. It can be seen that the surface is asymmetric. The global minimum is achieved when the wind capacity is 258.23 MW and the solar capacity is 153.29 MW.

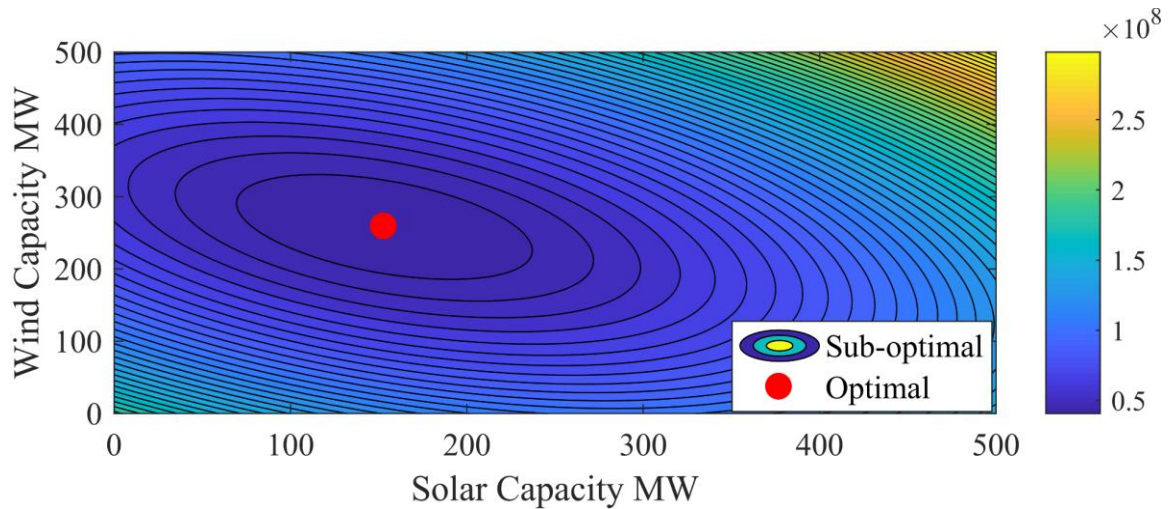


Figure 6.2. Graphical solution for unconstrained case

The values of wind and solar obtained in this unconstrained problem produce the following results in terms of power and energy:

Table 6-1. Results for the unconstrained case

Item	Power		Energy	
	MW	%	MWh/year	%
Load demand	192.10	100.0	1,240,400	100.0
Total VRE	411.52	214.2	966,598	77.9
Solar	153.29	79.8	247,544	20.0
Wind	258.23	134.4	719,054	58.0
Residual			-273,803	-22.1
Excess	158.37	82.4	107,976	8.7
Shortage	-178.17	-92.7	-381,779	-30.8

Regarding the results in terms of power, the total installed VRE capacity reaches 411.52 MW which is more than 2 times the maximum peak load demand. The wind installed capacity is 1.34 times the peak load demand, and the solar is 0.8 times. The wind-solar capacity ratio is 1.68.

In terms of residuals, the maximum excess power amounts to 158.37 MW which represents 82% of the peak demand. If the energy curtailment is kept to zero, this excess power must be stored by an equivalent size of storage system (158.37 MW). The maximum shortage

power reaches 178.17 MW or 92.7% of the peak demand. This shortage of power must be supplied by a combination of storage and dispatchable generation power capacity.

Based on the energy results shown in Table 6-1, the penetration of variable renewable energy sources reaches a value of 77.9% in terms of total annual energy. The wind generation has the largest share with 58% and solar generates 20% of the total energy.

The residual energy shortage of 30.8 % has to be supplied by either a dispatchable generator or an energy storage system. The residual energy excess reaches 8.7% which in practice must be stored or curtailed. Ideally, if all of it is stored, then a storage system with an annual energy capacity of 107,976 MWh/year is required, this energy will supply part of the residual energy shortage and a generator of 273,802 MWh/year will be needed.

6.3 Generator-Constrained Case

The total energy constraint shown in equation (29) forces the solver to find the wind and solar capacities that will supply the entire annual load demand energy, which reflects a scenario of 100% penetration of VREs. It also makes the residuals in the solution to have the same amount of residual energy excess and residual energy shortage. This means that a storage system can be charged with the excess residual and discharge that excess when needed to supply the shortage, ending up with a zero net residual value at the end of the year. Theoretically, there is no need for dispatchable generation in this case.

Annual energy constraint:

$$\sum_{t=1}^{8760} (W * F_W(t) + S_1 * F_{S1}(t)) \geq E_L \quad \forall t \quad (29)$$

Figure 6.3 shows the plot developed in Matlab for the objective function and the constraint function. In this case, the optimal solution must be on the constraint line, and the wind and solar capacities will increase to cover the total annual energy. The optimal is achieved with a wind capacity of 339.4 MW and a solar capacity of 182.9 MW which amounts to a total VREs installed capacity of 522.3 MW.

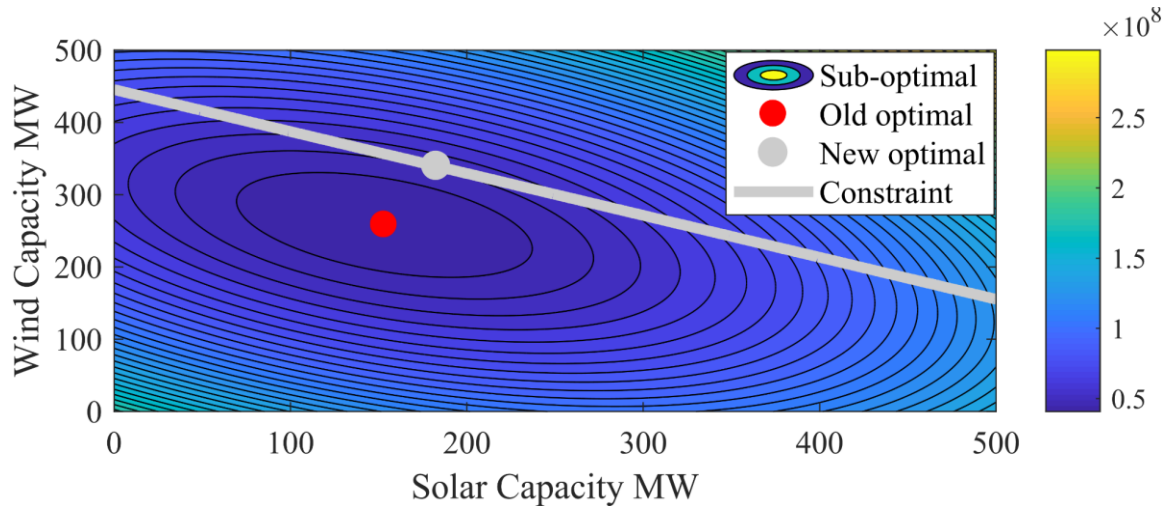


Figure 6.3. Graphical solution for the generator-constraint case

The values of wind and solar capacities obtained produce the following results in terms of power and energy:

Table 6-2. Results for generator-constrained case

Item	Power		Energy	
	MW	%	MWh/year	%
Load demand	192.10	100.0	1,240,400	100.0
Total VRE	522.29	271.9	1,240,400	100.0
Solar	182.88	95.2	295,324	23.8
Wind	339.41	176.7	945,076	76.2
Residual			0	0
Excess	243.37	126.7	277,360	22.4
Shortage	-176.15	-91.7	-277,360	-22.4

Regarding the results in terms of power, the total installed VRE capacity is 522.29 MW which amounts to 2.7 times the maximum peak load demand. The installed wind capacity

is 1.76 times the peak load demand, and the solar is 0.95 times. The wind-solar capacity ratio is 1.85.

In terms of power residuals, even though the residual energy is equal to zero when summing the whole year, not all hourly power residuals are zero. There is maximum excess power of 243.4 MW and a maximum shortage power of 176.1 MW. If the energy curtailment is kept to zero value, this excess power must be stored by an equivalent size of storage system (243.37 MW) and the shortage of power must also be supplied by this storage.

Based on the energy results shown in Table 6-2, the penetration of variable renewable energy resources reaches a value of 100% in terms of total annual energy. This is due to the constraint included in the optimization model that forces the total energy generated from wind and solar resources to be equal to the annual load demand. In this case, the wind generation has the largest share with 76.2% and the solar is 23.8%.

The remaining residual energy is zero. The energy excess with a value of 22.4 % supplies the energy shortage of -22.4 %. Ideally, this can be done with a storage system that charges with the excess and then discharges it to supply the shortage. Such a storage system will need to have an energy capability of 277,360 MWh/year.

6.4 Storage-Constrained Case

The constraint shown in equation (30) forces the optimization solver to find the wind and solar capacities for which any excess in generation will never exceed the predefined storage power capacity S .

Storage power constraint:

$$W * F_W(t) + S_1 * F_{S1}(t) - L(t) \leq S \quad \forall t \quad (30)$$

The values of wind and solar capacities obtained produce the following results in terms of power and energy:

Table 6-3. Results for storage-constrained case

Storage	Power (MW)					Energy (MWh/year)				
	Solar	Wind	Total VRE	Max. Excess	Max. shortage	Solar	Wind	Total VRE	Annual Excess	Annual Shortage
0	66.0	123.6	189.6	0.0	-184.6	106,574	344,238	450,812	0	-789,587
20	75.7	148.8	224.5	20.0	-183.6	122,229	414,341	536,570	883	-704,712
40	81.4	174.0	255.4	40.0	-182.6	131,490	484,444	615,934	5,554	-630,020
60	82.2	199.2	281.3	60.0	-181.9	132,672	554,548	687,220	16,481	-569,661
80	91.5	216.0	307.5	80.0	-181.1	147,798	601,401	749,199	29,754	-520,955
100	107.3	226.8	334.1	100.0	-180.4	173,253	631,425	804,678	44,173	-479,895
120	123.1	237.6	360.6	120.0	-179.6	198,710	661,446	860,156	62,472	-442,716
140	138.8	248.3	387.1	140.0	-178.9	224,163	691,473	915,636	84,461	-409,225
160	153.3	258.2	411.5	158.4	-178.2	247,544	719,054	966,598	107,976	-381,779
180	153.3	258.2	411.5	158.4	-178.2	247,544	719,054	966,598	107,976	-381,779

Regarding the results in terms of power, the total allowable installed VRE capacity increases as the storage power capacity increases. The maximum shortage of power capacity remains almost constant because there will be hours during the year with neither wind nor solar resources and regardless of the amount of installed wind and solar the result will be the same.

The energy generated by wind and solar resources goes up with the increase in storage size, increasing the renewable penetration in the system. With no storage, the penetration rate is 36.3% and with a storage of 160 MW or larger, the penetration reaches 78%. It is interesting to note that for storage sizes greater than 158.4 MW the wind and solar capacities remain constant.

6.5 Effect of Distributed Solar

For this case, the decision variable “solar” is split into central solar and distributed solar (≤ 500 kW) keeping the same onshore wind. This means that the optimization problem will have three decision variables instead of two.

The distributed solar has a slightly different hourly production profile than the central, with a higher capacity factor and smoother ramp rates in comparison to the central PV, as seen in chapter 4. However, the general shape of the production profile is similar to the central solar (the sun shines at the same time on the island), and consequently they cannot be directly optimized as independent variables because the solver solution will assign the maximum capacity to the distributed solar, leaving the central solar resources with a close to zero capacity value.

To overcome this issue, the distributed solar is added in the problem with an upper capacity constraint that limits the maximum installed capacity according to an estimation of how much distributed solar it is possible to have on the island by year 2030, taking into account the number of residential, industrial and commercial buildings.

Nowadays, Barbados has a distributed solar installed capacity close to 20 MW [35] [36]. Assuming the amount of distributed solar would increase on the island up to a maximum value of 50MW [35] by year 2030, we can run the optimization model for different levels of distributed solar to compare the results.

To observe the effect of adding distributed solar capacity in the optimization, the results will be compared with the unconstrained case, in section 6.2. The results in terms of power values are shown in Table 6-4 and in terms of energy in Table 6-5.

Table 6-4. Power results for different levels of distributed solar PV

Item	Power MW				
	Distributed Solar PV				
	0 MW	20 MW	30 MW	40 MW	50 MW
Total VRE	411.52	409.76	408.88	407.99	407.11
Wind	258.23	257.02	256.41	255.80	255.19
Total Solar	153.29	152.74	152.47	152.19	151.92
Central Solar	153.29	132.74	122.47	112.19	101.92
Distributed Solar	0.00	20.00	30.00	40.00	50.00
Residual					
Excess	158.37	158.24	158.17	158.10	158.04
Shortage	-178.17	-171.15	-171.00	-171.02	-171.03

As seen in Table 6-4, adding 50 MW distributed PV is marginally beneficial in terms of the total power capacity required reducing it by 4.4 MW.

For every capacity value of distributed solar added, the central solar capacity is reduced by the same amount or more. This corroborates the assumption that these two variables are dependent.

The maximum excess power residual does not vary significantly. The maximum shortage power residual is reduced by around 7 MW which means less dispatchable generation capacity will be needed.

Table 6-5. Energy results for different levels of distributed solar PV

Item	Energy MWh/year				
	Distributed Solar PV				
	0 MW	20 MW	30 MW	40 MW	50 MW
Total VRE	966,598	968,216	969,025	969,833	970,642
Wind	719,054	715,665	713,970	712,275	710,580
Total Solar	247,544	252,551	255,055	257,558	260,062
Central Solar	247,544	214,364	197,774	181,184	164,594
Distributed Solar	0	38,187	57,281	76,374	95,468
Residual	-273,803	-272,185	-271,375	-270,566	-269,757
Excess	107,976	106,928	106,479	106,100	105,783
Shortage	-381,779	-379,113	-377,854	-376,666	-375,540

Table 6-5 shows the results in terms of energy. The total VRE generation increases by 4,044 MWh/year when adding the distributed solar. The main driver for this increase is the solar generation that goes up by 5% or 12,518 MWh/year in comparison to the scenario without distributed solar. The wind generation decreases by 8,474 MWh/year because the installed capacity was reduced according to Table 6-4.

In terms of residual energy, adding distributed solar is beneficial because it reduces the amount of residual energy by 4,046 MWh/year, with a 2,193 MWh/year reduction in excess energy and 6,239 MWh/year reduction in shortage energy. By decreasing this energy excess and shortage, the system will indirectly reduce the later storage and dispatchable generation usage.

In summary, the inclusion of distributed solar in the model improves the results by a small margin and makes the final numbers more accurate, although it has to be included with the predefined value of 50MW. The distributed solar PV will be considered in the following optimization models as a predefined value.

6.6 Effect of Load Demand

Several load demand profile estimations are available for the year 2030 in Barbados as detailed in chapter 3.

Using the unconstrained optimization model from section 6.2, and evaluating the 12 different load profiles shown in Table 6-6, it is possible to visualize the effects of using different load demand forecasts.

Table 6-6. Load demand scenarios

Scenario	Load	EV Load
1	Low	No EV
2	Medium	
3	High	
4	DSM	
5	Low	Home Charging EV
6	Medium	
7	High	
8	DSM	
9	Low	Work Charging EV
10	Medium	
11	High	
12	DSM	

To carry out this analysis, the optimization is run for all 12 load demand scenarios, the distributed solar PV is set to 50MW, and the central solar PV and onshore wind are determined by the solver. The numerical results are shown in Appendix A, and the following figures summarize the results found.

Figure 6.4 shows the optimal wind and solar capacities obtained in the optimization for the 12 different load demand scenarios. It can be seen that the required VRE capacity increases when the load demand is higher. The load demand with Demand Side Management (DSM) technologies requires the least renewable capacity, and the high demand scenario requires the most. In general, having a high load demand will require 1.8 - 2.26 times more VRE capacity than having a low demand scenario with DSM.

When adding the EV load demand, the required wind and solar capacities increase as well. However, the type of charging profile changes the wind-solar proportion. Home charging increases the need for wind power capacity because the EV load rises during the evenings when people arrive at home, and work charging increases the need for solar power capacity

as the cars are charged during the daytime when there is sunlight, and solar facilities generate electricity.

Figure 6.5 shows the results in terms of the total energy generated in the year. The energy generated is proportional to the installed power capacity of wind and solar. Therefore the pattern is similar to Figure 6.4.

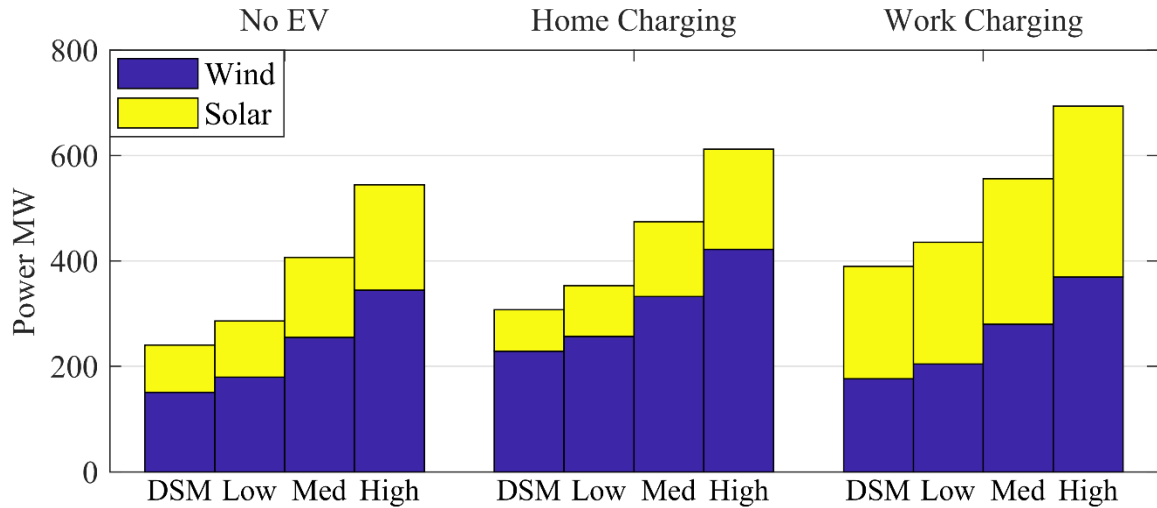


Figure 6.4. Effect of load demand on the optimal wind and solar power capacities

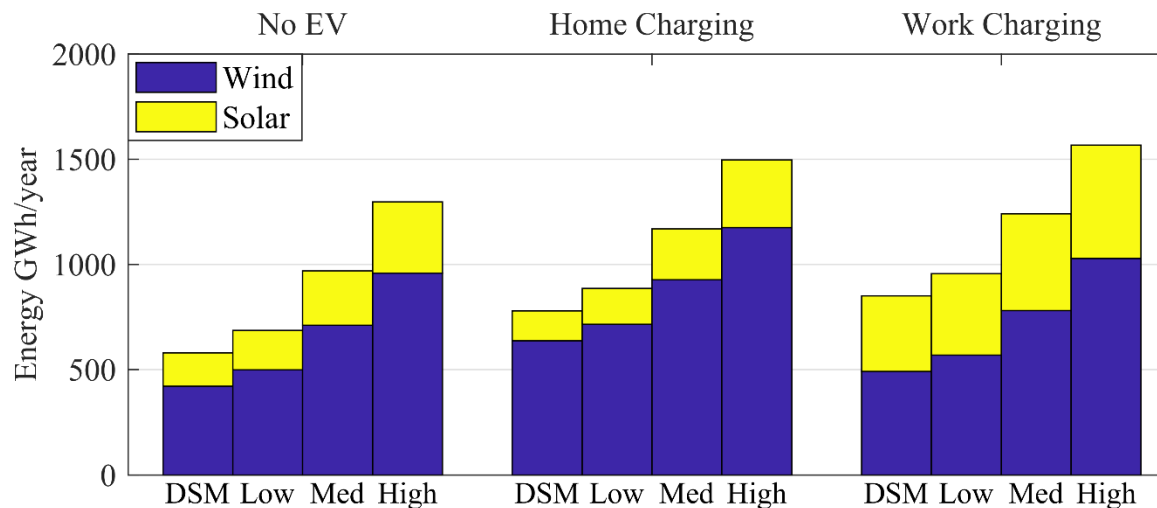


Figure 6.5. Effect of load demand on wind and annual solar energy generated

Figure 6.6 shows the excess and shortage power residual for the 12 load demand scenarios. The largest residual power shortage is present when the load demand is high, and when the EVs are charged at home. This happens because during the evenings the solar generation goes down and the load demand usually increases. If the EVs are charged in this period, the load demand will increase even further, creating a larger shortage power residual. The best case is the scenario with DSM technologies and no EVs or work charging EVs.

Figure 6.7 shows the annual residual energy excess and shortage. In practice, the excess energy must be stored in a storage unit, and the shortage of energy must be supplied by a combination of dispatchable generation and storage. The highest energy shortages and excesses occur when the load demand is high and there is home charging EVs present.

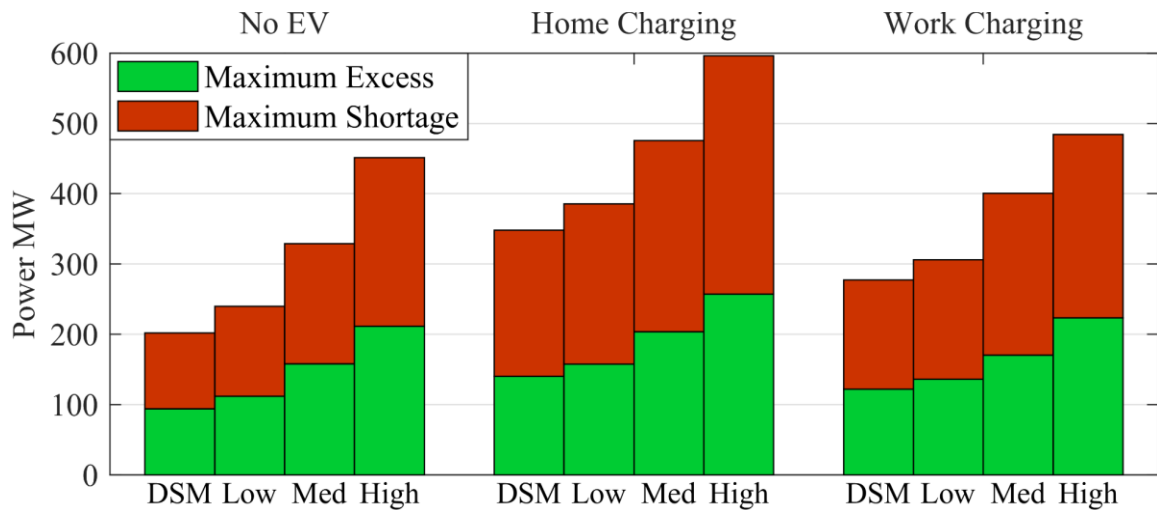


Figure 6.6. Effect of load demand on maximum excess and shortage power residual

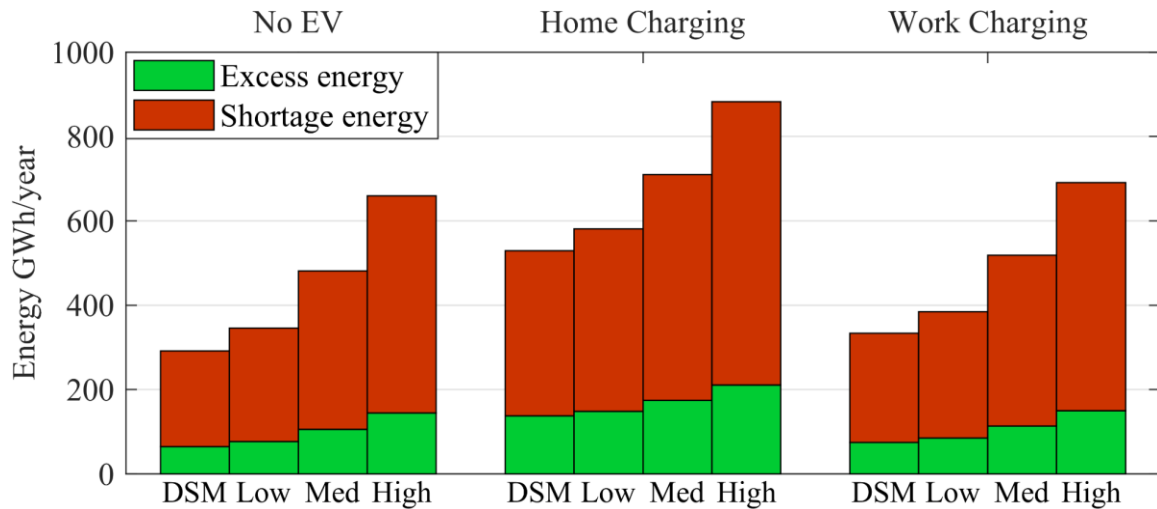


Figure 6.7. Effect of load demand on wind and solar annual residual energy

6.7 Selected Scenarios

After determining the effects of different constraints and inputs to the optimization model in the previous sections, only the extreme cases are selected to carry the results to the next optimization model, where the storage energy capability and dispatchable generation capacity are optimized.

The wind and solar are optimized using the residual optimization model which mathematical formulation is shown in section 5.2.3 with the constraint on the maximum residual power excess, for every hour. This constraint allows the values for storage power capacity S , to be predefined as an input parameter.

The distributed solar PV is set to 50 MW, and the load demand scenarios considered are only the extreme cases shown in Table 6-7. Scenario 4, with the DSM load and no electric vehicles, gives the lowest wind and solar power capacities as a result. Scenario 7, with the high load and home charging EVs, gives the highest residuals in the results which will have to be covered by dispatchable generation and storage. Finally, scenario 11, with high load demand and work charging EVs, gives the highest solar and wind power capacities.

Table 6-7. Selected load demand scenarios

Selected Scenarios	Load Profile	Energy	Peak	Average	Lowest	Load factor
		MWh/year	MW	MW	MW	%
4	DSM Load + No EV	742,500	115.1	84.8	51.4	73.6
7	High Load + Home Charging EV	1,957,752	347.2	223.5	116.9	64.4
11	High Load + Work Charging EV	1,959,215	354.6	223.7	124.4	63.1

Now, these three cases are run in the optimization solver with different values of storage power in the constraint. The results are shown in Appendix B and summarized in the following figures.

Figure 6.8 and Figure 6.9, show the optimal solar and wind power capacities obtained in the solution. The results represent the minimum and maximum values of installed power capacities required on the island. Any values between the lower and upper lines contain the solutions for the other load demand scenarios.

The amount of wind and solar capacities in the solution increase with the rise of storage power capacity. This is because storage allows the integration of more variable renewable resources. However, there is one point for each scenario at which the curve saturates. After the saturation point, no matter how much storage power capacity is added the amount of wind and solar capacities remain constant.

It is also possible to conclude that EVs have a significant impact on the results. With work charging EVs, the system requires more solar power capacity and less wind because the cars can be charged during the day with the solar generation. With home charging EVs, the system needs the opposite, more wind and less solar.

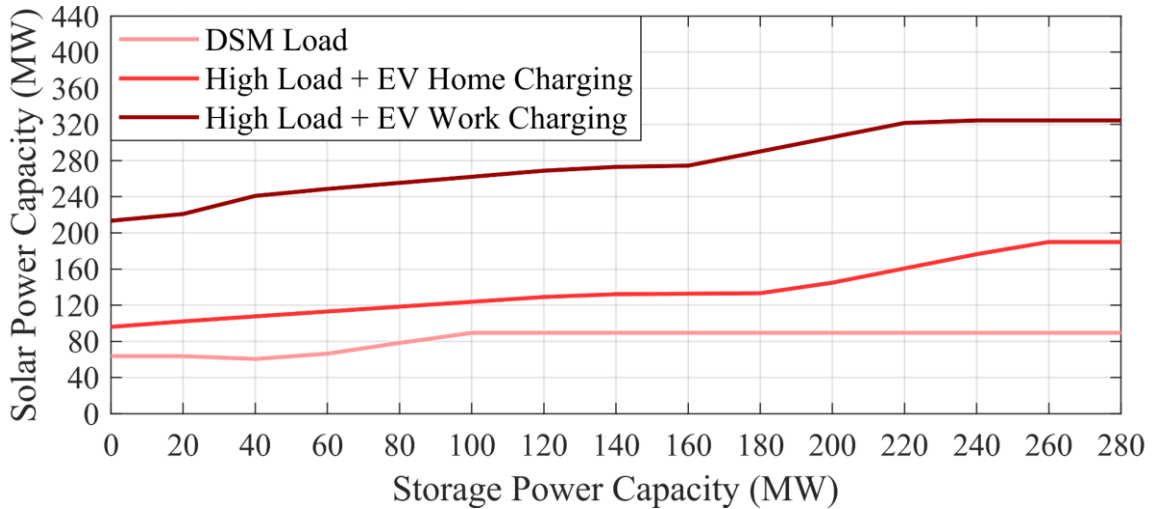


Figure 6.8. Optimal solar power capacity versus storage power, for the three load demand scenarios

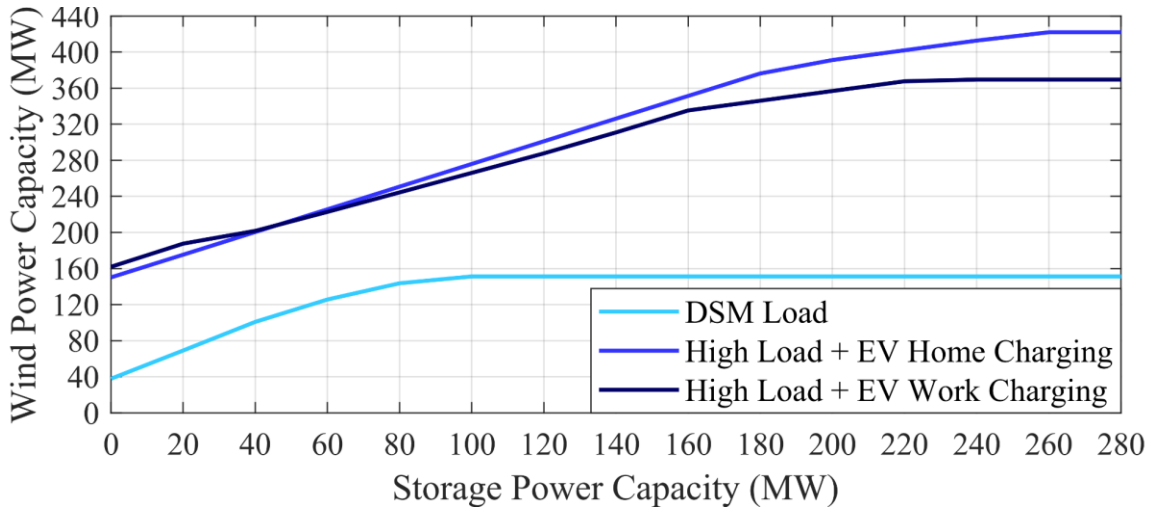


Figure 6.9. Optimal wind power capacity versus storage power, for the three load demand scenarios

Figure 6.10 shows the total wind plus solar capacity versus the storage power. Three conclusions can be drawn from here.

First, the higher the storage power capacity in the system the more VRE can be integrated. Second, there is a different saturation point for every load demand scenario. For the lowest load demand, saturation is reached at 244 MW, and for the other two scenarios the saturation point is reached at higher values.

Third, the load demand with work charging EVs requires the most VRE power capacity because solar capacity is demanded to charge the cars during office hours when the solar generation is available.

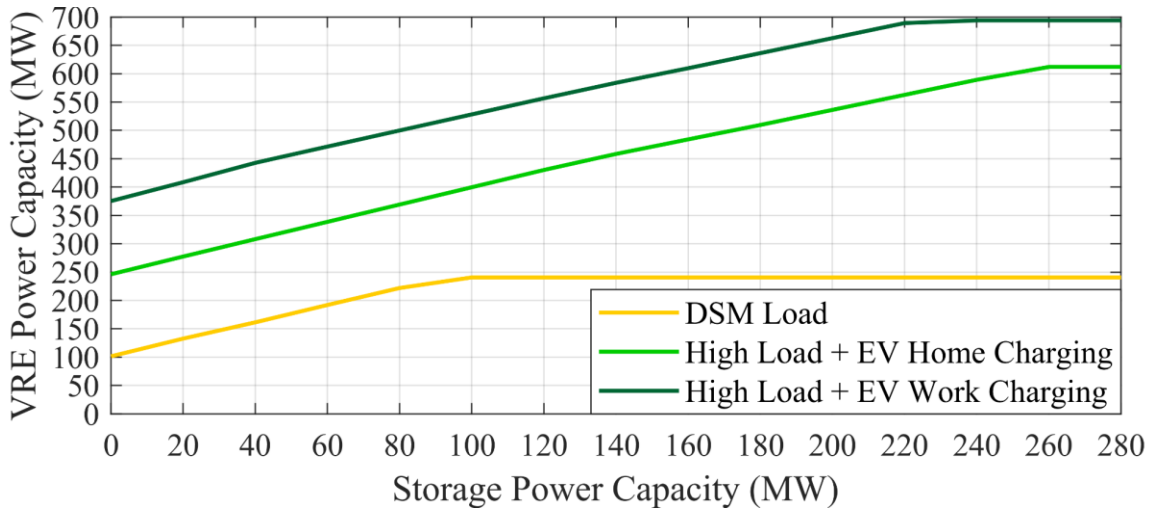


Figure 6.10. Optimal VRE capacity versus storage power, for the three load demand scenarios

Figure 6.11 shows the results in terms of the residual energy accumulated during the year. In this category, the high load demand with home charging EVs has the highest residual energy shortage and excess. This increases the need for dispatchable generation and storage to cover those residuals in the next cost optimization model.

The residual energy excess must be stored in a storage unit to avoid curtailment of free energy. The residual energy shortage must be supplied by a combination of dispatchable generation and storage.

The increase in the storage power capacity reduces the accumulated residual energy shortage until a saturation point is reached but increases the accumulated residual energy excess.

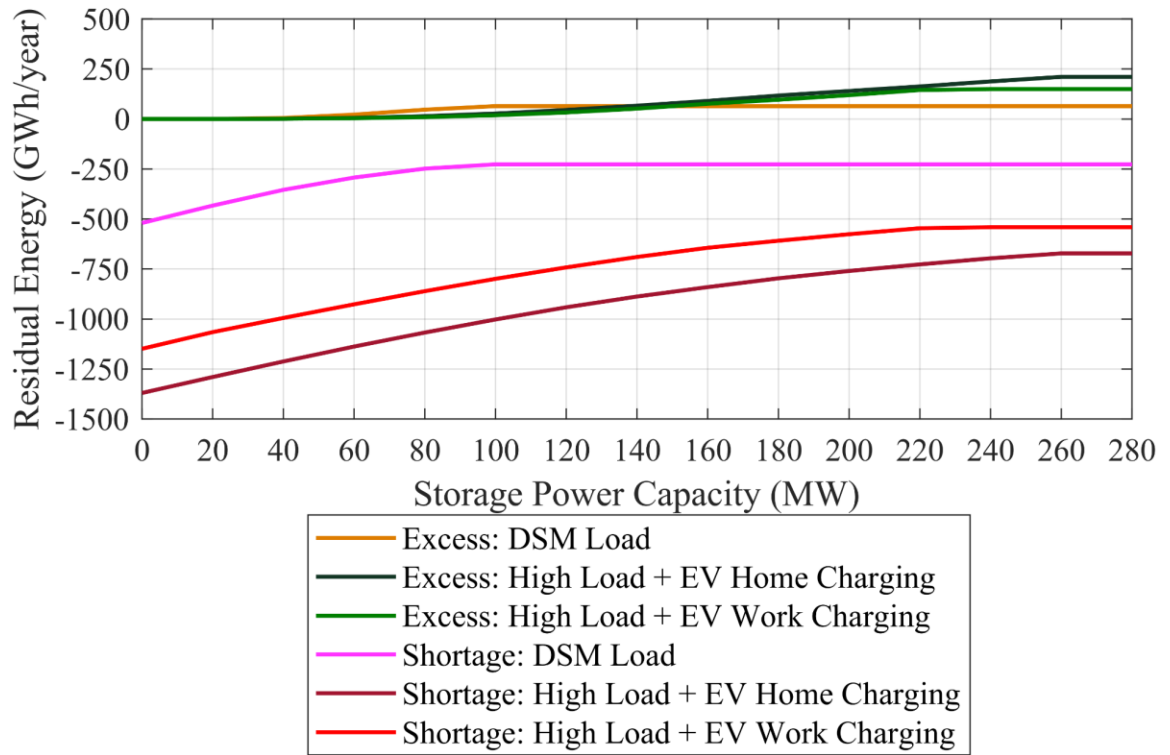


Figure 6.11. Annual generation excess and shortage versus storage power, for the three load demand scenarios

7 Cost Optimization of Wind and Solar

7.1 Introduction

In this section, the results of wind and solar obtained with the cost optimization model are shown and compare to the previous residual optimization results.

7.2 Results

The costs of wind and solar technologies considered for this model were obtained from the Emera 100/100 vision for Barbados report [37].

$$\text{Solar} = 2.05 \text{ Million USD/MW}$$

$$\text{Wind} = 2.50 \text{ Million USD/MW}$$

Figure 7.1 represents the objective function solution space. It can be seen that the solution tends to go to zero wind and zero solar capacity values because of the slope of the plane. Figure 7.2 is the projection of the curve in the two dimensional plane of wind and solar power capacities, and the green point on it represents the optimal solution for this unconstrained case, which occurs at the origin.

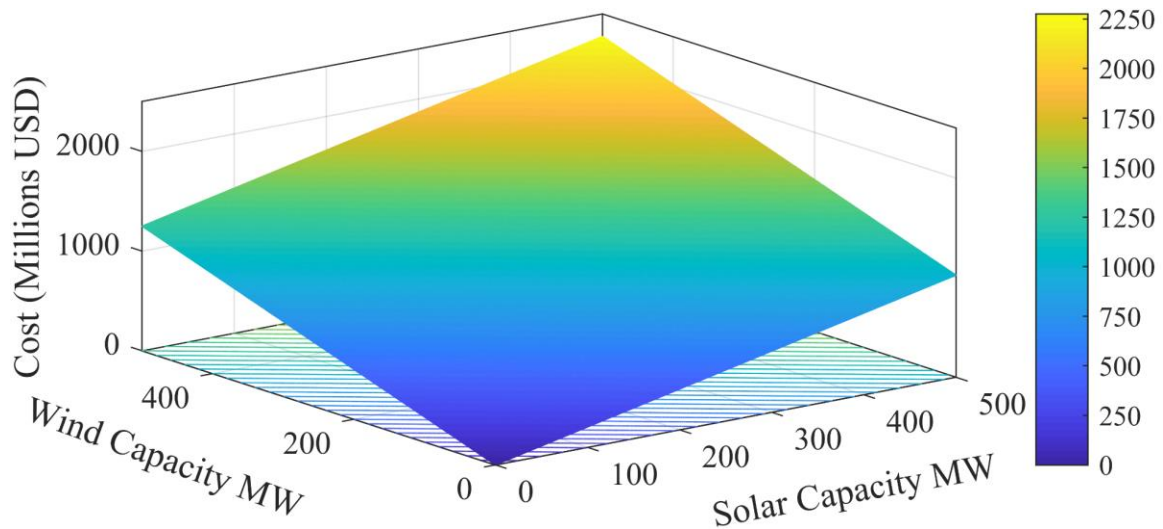


Figure 7.1. Three dimensional representation of objective function

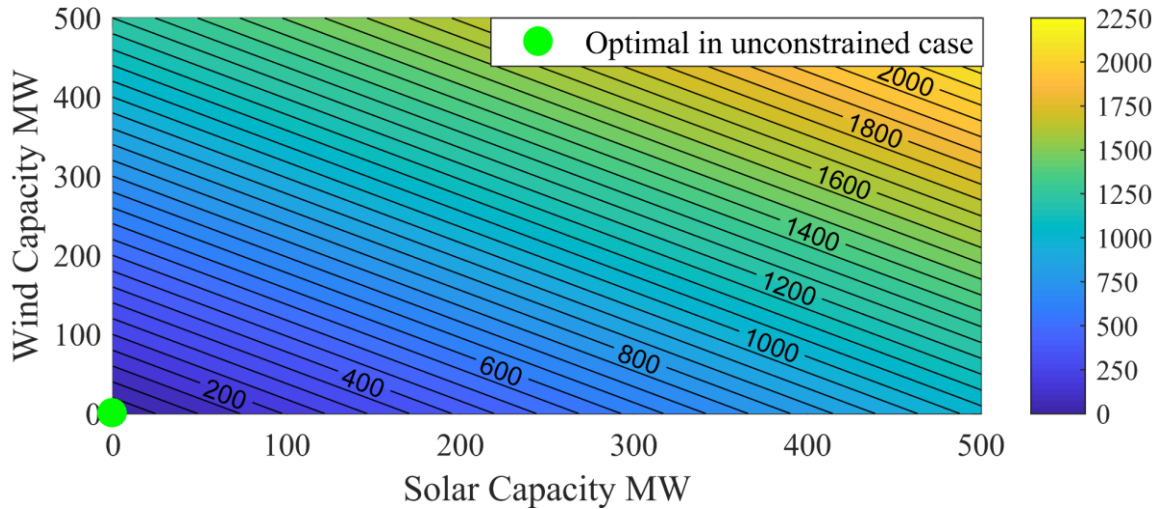


Figure 7.2. Contour plot of the cost objective function solution space

Because of the constraints included in the problem, the solution depends on the values of renewable penetration level and the storage power capacity. The optimization is run for several values of storage from 0 to 280 MW and several levels of penetration from 50% to 100%, using the medium load demand without EVs as a reference case.

Figure 7.3 shows the results for this cost optimization. The colored background represents the total cost of any possible combination of wind and solar in millions of dollars. The pink lines are the storage hourly constraints shown in the equation (6) of the mathematical formulation. These constraints are 8760 in total, representing every hour of the year, however, for simplicity, only the 2-3 more restricting hours (lines) are shown in the figure for every value of storage power. The solution is forced to be on or below these pink lines. The cyan lines represent the annual energy constraint shown in equation (7) of the formulation. Each line represent a desired percentage of renewable energy penetration. The solution is forced to be on these lines.

Therefore, the cost optimization chooses the solution with the lower cost according to the total cost represented in the colored background, below or on the pink lines depending on the storage value and on the cyan line depending on the desired renewable penetration.

According to the results, It can be seen that the cost optimization is not very effective because the solutions tend to have more wind capacity and they quickly go to the extreme on the y-axis, leaving the system with zero solar capacity.

The solution for the residual optimization using 160MW of storage is shown on the figure for reference. It can be calculated that for the same storage value, the cost of the residual solution is 45 Million USD more expensive than the solution from the cost optimization. The residuals-based solution requires 153.29 MW of solar and 258.23 MW of wind. In contrast, the cost optimization requires 54.03 MW of solar and 325.04 MW of wind.

The cost optimization is based only on capital costs because wind and solar have no fuel cost. The figure obtained from the cost optimization model can be employed to visualize the cost sensitivity of different combinations of wind and solar with different renewable penetration levels and different storage power capacities.

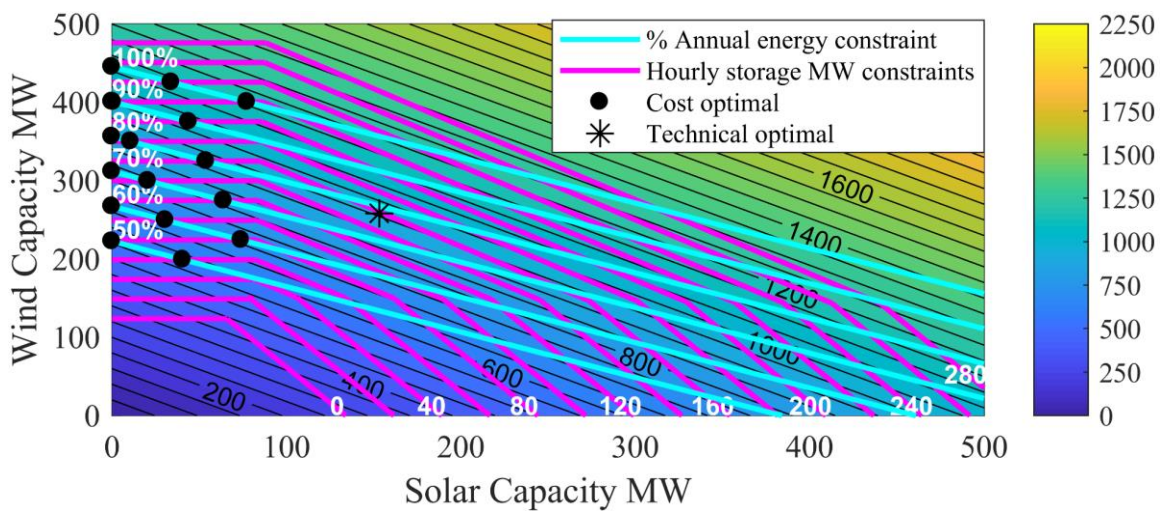


Figure 7.3. Cost optimization results for different values of storage and renewable level

8 Cost Optimization of Dispatchable Generation and Storage

8.1 Introduction

In this section, the results for the optimal values of dispatchable generation capacity and storage energy capability are shown.

The first section, shows the results in terms of capacity and energy under different load demand profiles, storage power capacity and energy curtailment. A total of 90 model runs are summarized in the results.

The second section, shows the operational results of the system to visualize the interaction of the different units during the year. An example case is shown as reference.

Figure 8.1 shows the LINGO solver status for this model. The solver takes approximately 34 seconds and 30,433 iterations to reach the optimum global value. The model contains 43,802 variables and 122,649 constraints.

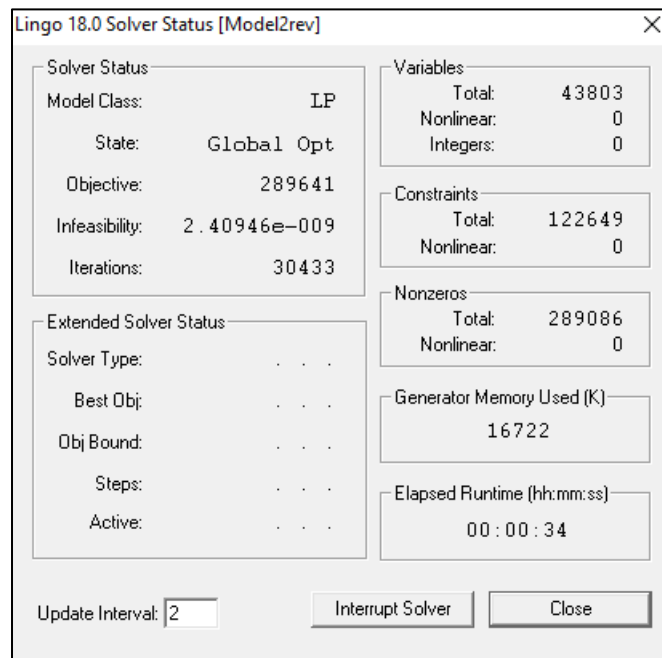


Figure 8.1. Optimization solver status

8.2 Technology costs

The main purpose of this research work is to develop the cost optimization model that will allow decision makers in Barbados to choose the optimal capacities for the all-renewable power system. Therefore, the costs presented here are from references and can be changed at any time to adapt to local costs on the island and to time. In this work, the costs used for the system are:

Biomass [38]:

Capital cost CC_G = 4.985 Million USD/MW

Operational cost CO_G = 4.2 \$/MWh

Storage Lithium-Ion [39][38]:

Power capacity cost CC_S = 2.4 Million USD/MW

Energy capability cost CC_H = 0.65 Million USD/MWh

Operational cost CO_S = 8 \$/MWh

8.3 Capacity Results

The results presented in this section represent 90 model runs to compare the results under different levels of storage power, load demand and curtailed energy. The storage power and load demand scenarios are the same as used in the residual optimization for wind and solar. The amount of curtailed energy allowed is introduced as a variable, to compare the results without curtailment and with a 10 % curtailment.

Figure 8.2 shows the optimal capacity for the dispatchable generation unit under the different scenarios. Four conclusions can be drawn from the results shown in this figure.

First, the generator installed power capacity decreases with the addition of storage power in the system, until a point of saturation which depends on the load demand scenario. When

adding storage the residual shortage power is supplied by a combination of storage and generator installed power capacity.

Second, the lower the load demand, the less generation power capacity required. The highest load demand scenario requires around three times more generation installed power capacity than the lowest demand scenario (DSM load) for low values of storage.

Third, having home charging EVs in the load requires a larger generator power capacity. This is because work charging EVs can use the electricity coming from solar generation during the day and home charging EVs cannot, requiring a larger dispatchable power capacity to compensate when there is not enough wind capacity.

Fourth, allowing some energy curtailment in the system increases the generator installed power capacity required.

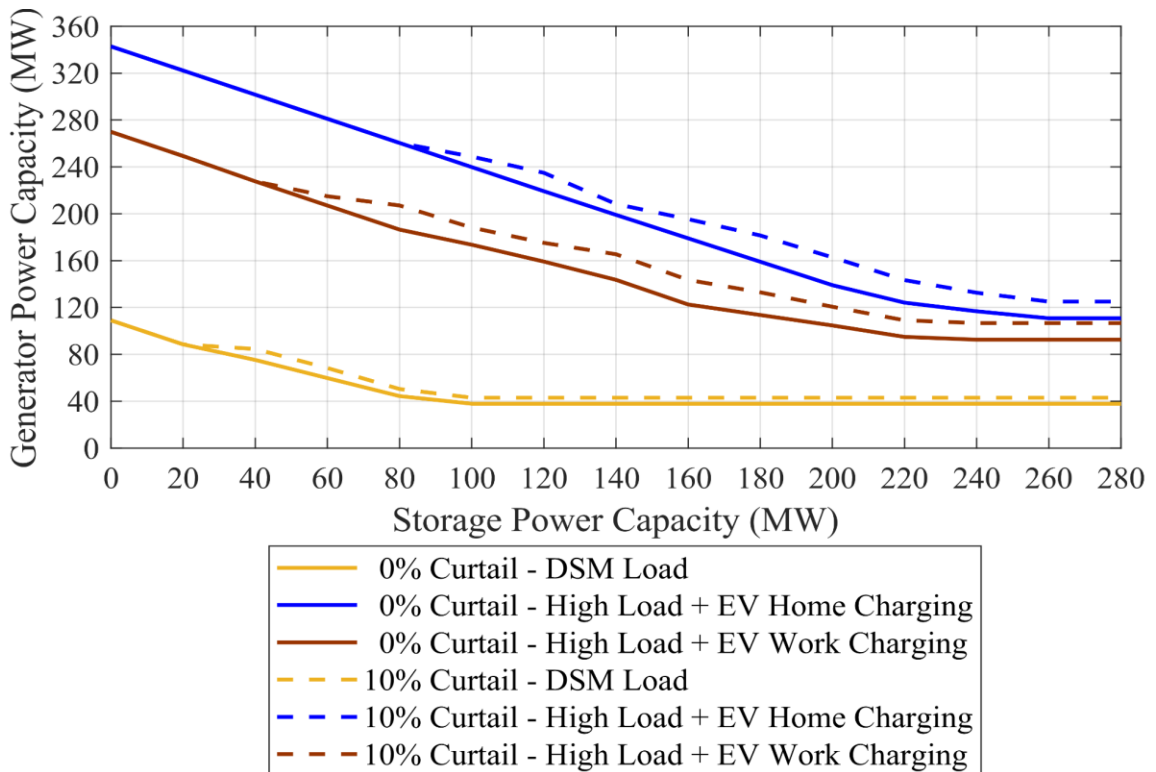


Figure 8.2. Optimal generator power capacity for different levels of storage power, load demand and curtailed energy level

Figure 8.3 shows the optimal storage energy capability under the same scenarios. Four conclusions can be drawn from this figure.

First, increasing the storage power capacity rapidly increases the storage energy capability required in the system until a saturation point. This happens because the higher the storage power capacity, the more hourly excess is allowed to be stored at every time interval. Consequently, larger blocks of energy accumulate in the storage unit.

Second, the storage energy capability required is smaller when the load demand is lower. The storage energy capacity can be up to 2.6 times greater when comparing the highest load demand against the lowest load demand scenario (DSM load).

Third, work charging EVs require more storage energy capacity than home charging. This is opposite to the generator capacity results, where the capacity needed was higher for the load with home charging EVs. The storage energy capacity is bigger for work charging because the system has more solar capacity and therefore has more excess residual energy during the daytime that needs to be stored.

Lastly, allowing some curtailment of energy significantly reduces the size of the storage energy capacity required in the system. By allowing 10% of annual curtailed energy, the storage energy capacity required can be reduced 2.5 times.

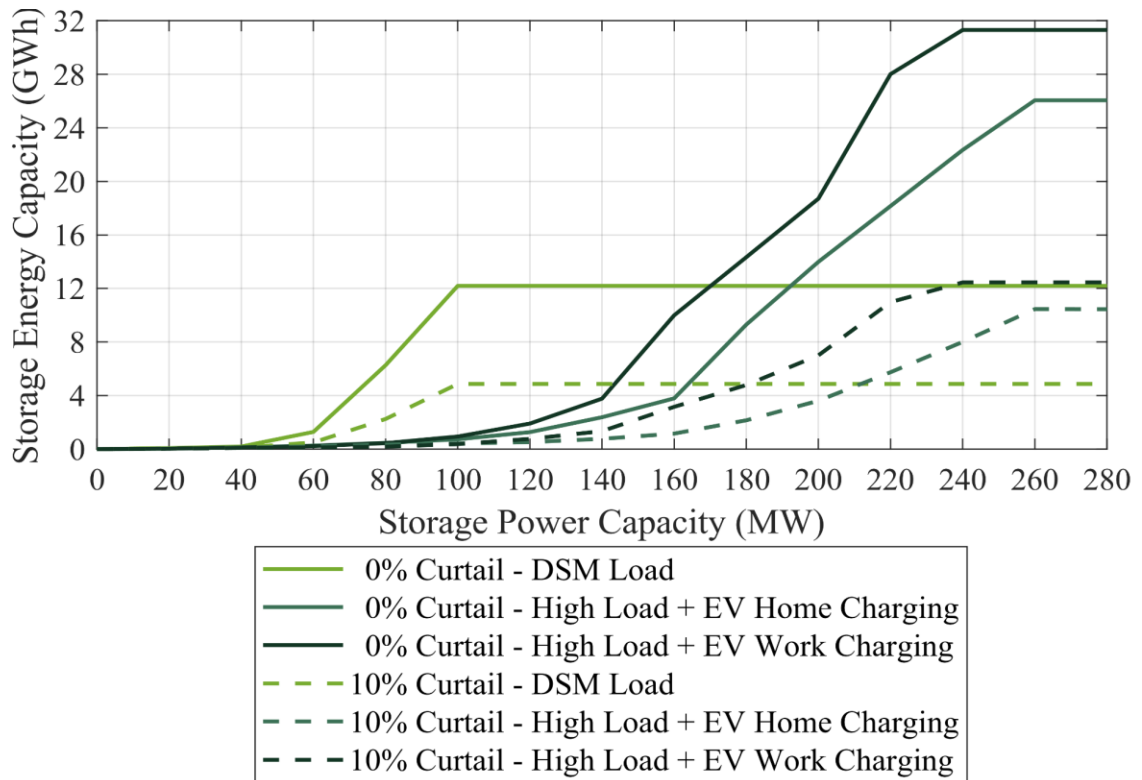


Figure 8.3. Optimal storage energy capacity for different levels of storage power, load demand and curtailed energy level

Figure 8.4 shows the annual energy generated by the dispatchable unit. From the figure we can conclude the following:

First, increasing the storage power capacity decreases the annual dispatchable generation until a saturation point.

Second, the annual dispatchable generation is less when the load demand is lower. For the highest load demand scenario, the annual generation can be up to 2.7 times greater than in the lowest load demand scenario (DSM load).

Third, having home charging EVs in the load requires more annual dispatchable generation than having work charging. This is because work charging EVs can use the electricity coming from solar generation during the day and home charging EVs cannot, requiring a

dispatchable generation to compensate when there is not enough wind generation. It can be estimated that 20% more dispatchable energy generation is necessary when having home charging instead of work charging EVs.

Fourth, with curtailment of energy in the system the annual dispatchable energy generation increases to make up the curtailed energy difference.

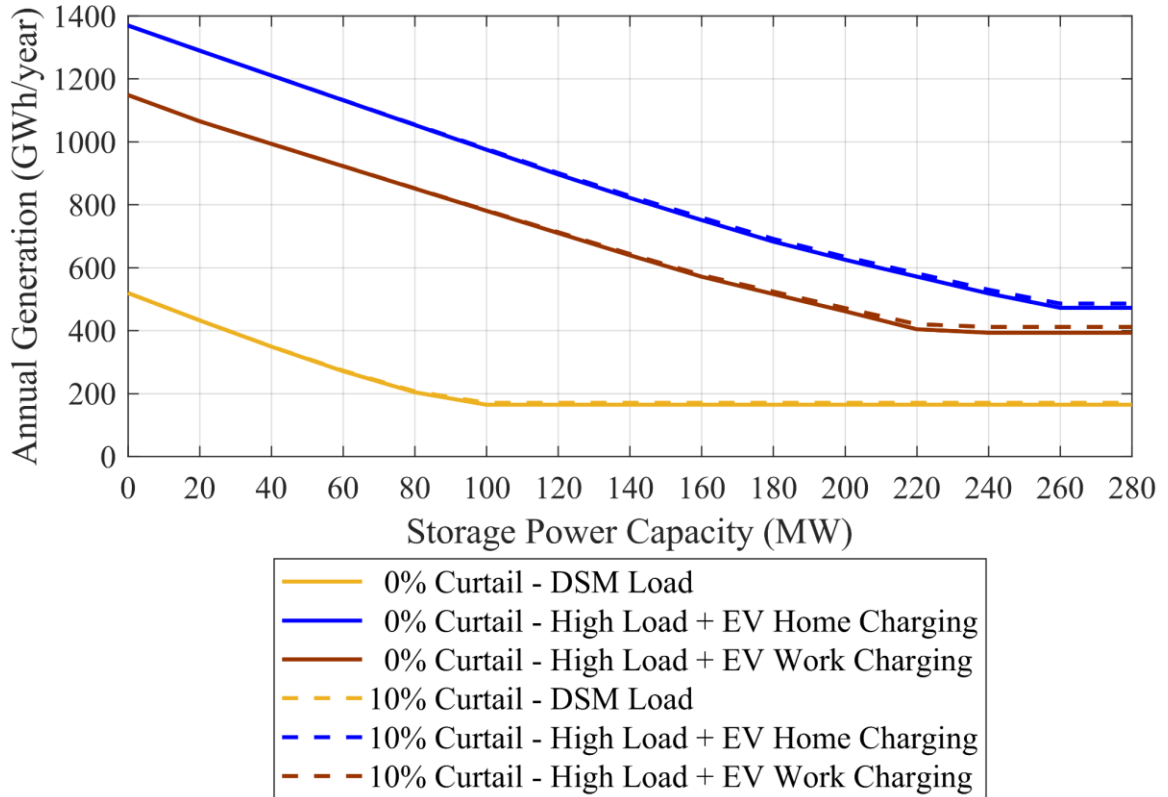


Figure 8.4. Annual Dispatchable generation for different levels of storage power, load demand and curtailed energy level

Figure 8.5 shows the 10% curtailed energy values used for every scenario. The curtailed energy is higher for scenarios with higher residual energy excess. The scenarios with higher residual energy excess are the ones with larger storage power capacities.

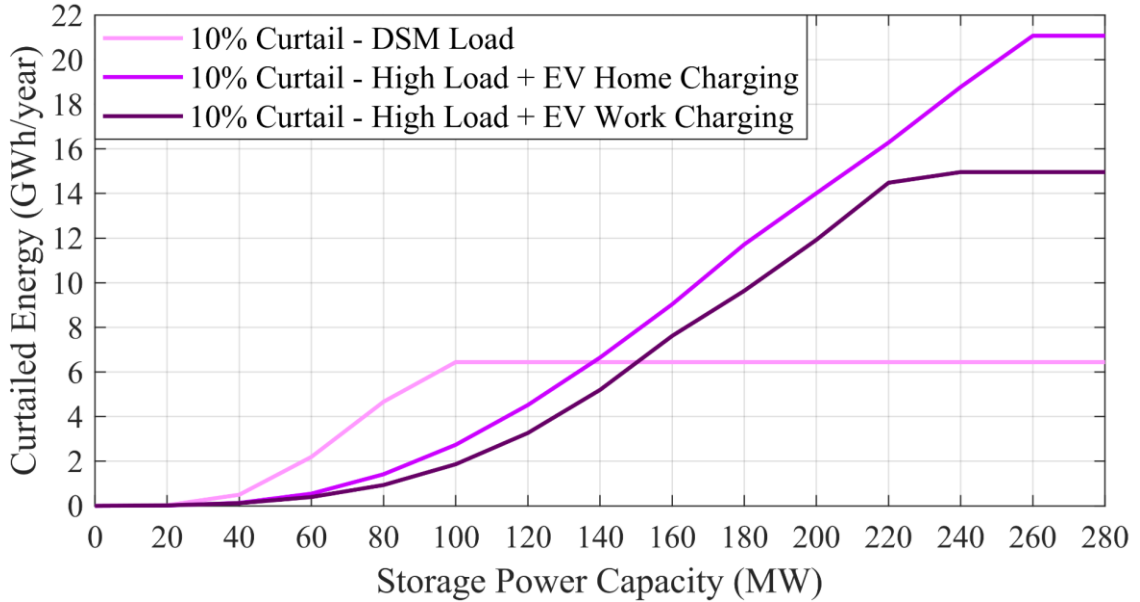


Figure 8.5. 10% curtailed energy for different levels of storage power and load demand

8.4 Operational Results

The cost optimization model estimates an operational dispatch to supply the load demand at all times, under certain operational constraints. This operational result allows the model to obtain the optimal generation and storage capacities shown in the preceding section.

As a consequence, the hourly operation dispatch is available for the 90 model runs presented previously. However, only one case is shown here as a reference. This scenario corresponds to high load demand, home charging EVs, 160MW storage and with zero energy curtailment.

Figure 8.6 and Figure 8.7 show the residual values coming from the optimization of wind and solar capacities in the residual optimization model. These residuals must be supplied or stored at every time interval to avoid unserved energy. For this case the optimal wind power capacity is 351 MW and the solar power capacity is 132.7 MW.

The remaining figures show the hourly power dispatch of the dispatchable unit, the storage power discharge and charge, and the energy state of charge of the storage. For this case the optimal generator capacity is 179 MW and the storage energy capacity is 3,790 MWh.

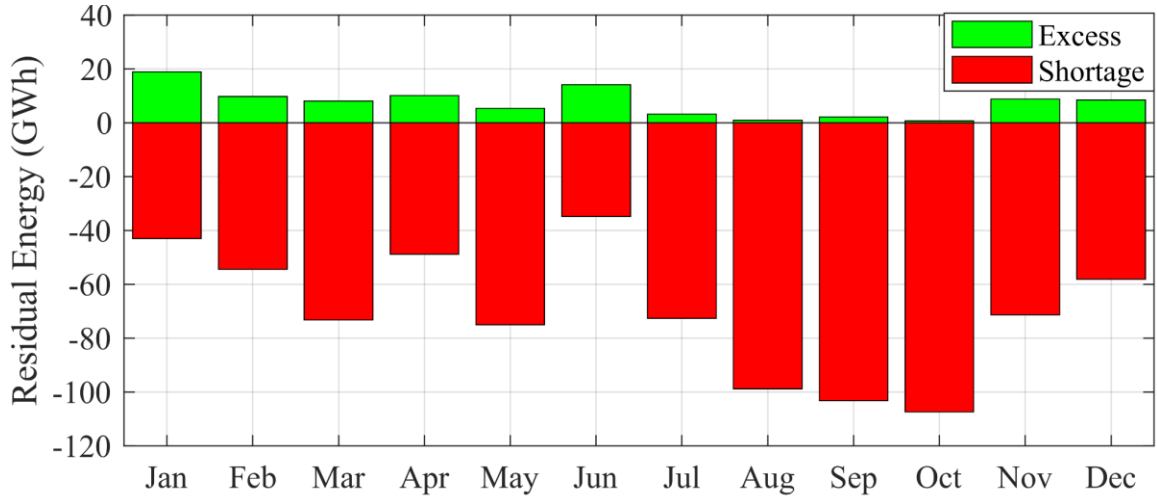


Figure 8.6. Monthly energy residuals for example case scenario

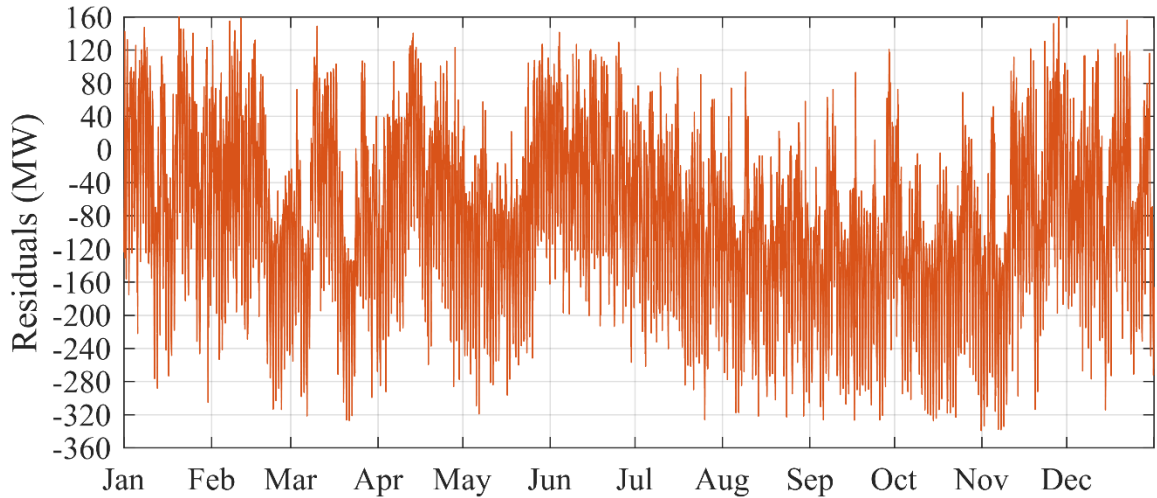


Figure 8.7. Hourly power residuals for example case scenario

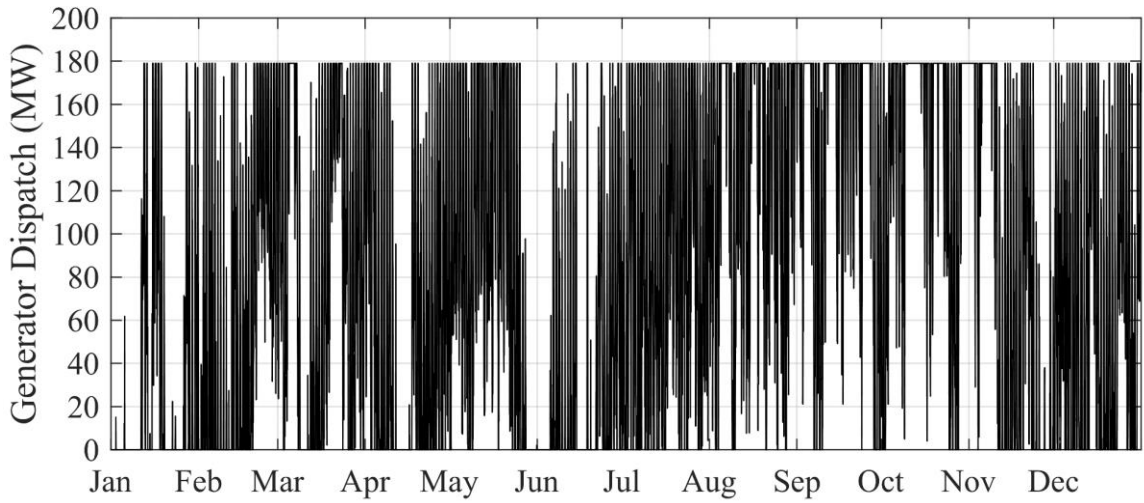


Figure 8.8. Optimal hourly generation power dispatch for example case scenario

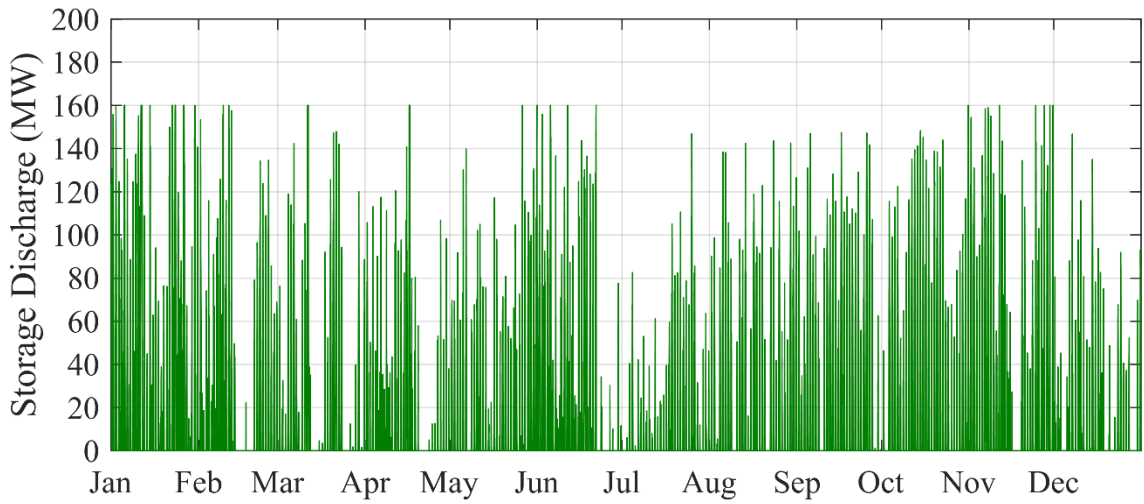


Figure 8.9. Optimal hourly storage power discharge for example case scenario

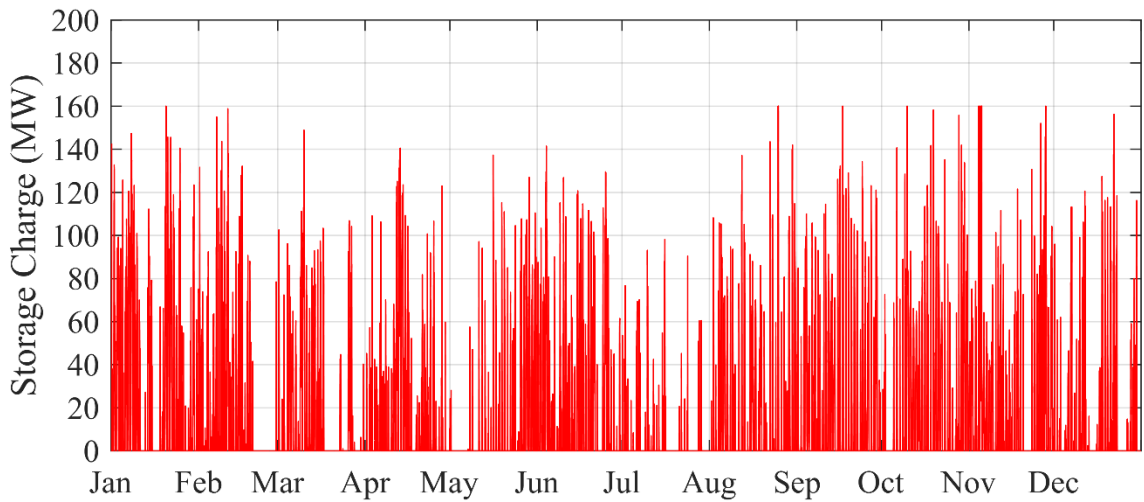


Figure 8.10. Optimal hourly storage power charge for example case scenario

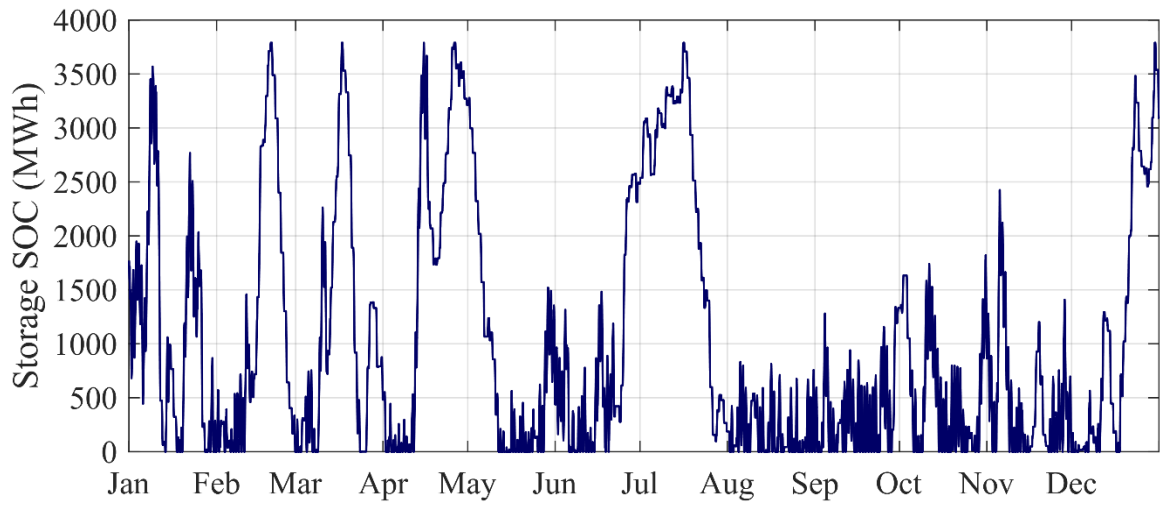


Figure 8.11. Optimal hourly storage state of charge for example case scenario

9 Conclusion

9.1 Results and Discussion

The results of this research work provide a framework for Barbados on how to obtain a 100 per cent renewable generation power system, indicating how much generation capacity and the optimal mix that they need to have by year 2030. The study cases evaluated throughout this document do not provide a single solution, but instead set the boundaries for the optimal generation capacities under different scenarios. This gives a certain degree of freedom to decision-makers on the island so they can choose the solution that best represents more specific and local requirements.

Regarding the methodology used, several significant conclusions can be extracted. The most important one is the fact that this methodology can be applied to any small islanded power system that wants to study their alternatives in terms of 100 per cent renewable energy penetration.

The concept of residuals becomes relevant when having considerable amounts of variable renewable generation such as solar and wind because these resources are non-controllable and intermittent in nature.

The residual optimization model successfully obtains the optimal values of wind and solar capacities under different scenarios. It provides a simple, straightforward and easy to understand method that gives plenty of flexibility to run different scenarios.

The residual optimization model also shows that it is possible to indirectly minimize the need for storage and dispatchable generation that will support the wind and solar integration.

The main limitations of this method are two. First, it does not allow the optimization of dependent renewable resources. For example, if central and distributed solar are to be used in the model, the power capacity of one of the resources must be predefined so that the other can be optimized. This happens because the solar sunlight resource on the island is the same for both solar generation technologies, especially as Barbados is geographically small. The second limitation is that the results vary when using renewable resources with different capacity factors. Therefore, the models should be re-run to update the optimal generation capacities if different capacity factors are to be used.

The cost optimization model for wind and solar shows that the optimal values tend to go to the extremes, favoring large amounts of wind capacity over solar in the solution. However, the cost model is useful as a reference to determine the cost variation for any combination of wind and solar obtained in the residual optimization model and it helps to visualize how far from the optimal cost is the technical solution.

The cost optimization model for storage and dispatchable generation, although more complex and sensitive to variations in the formulation than the first one, provides the optimal generation and energy storage capacities.

Concerning the combined results of both optimization models, the relationship among the different renewable resources is clear and consistent. The more storage power capacity, the more solar and wind can be integrated into the system and the smaller dispatchable generation power capacity is required to support the integration. However, the storage energy capacity in MWh increases to absorb the greater amount of excess energy residuals. Using different load demand forecasts significantly affects the results. Having a low demand forecast results in lower wind and solar capacities, lower dispatchable generation

power capacity and lower energy storage capability in the system. Therefore, it is important that Barbados makes sure to use the right load demand scenario to plan the renewable generation capacities for the year 2030.

The integration of DSM technologies reduces the peak load demand of the system, and the optimization results show a reduction in the optimal capacities of all the generation resources: wind, solar, dispatchable generation and energy storage.

Electric vehicles also affect the results of the optimization because they add load to the system. However, the magnitude of the effect depends on the charging strategy to be used for the electric vehicles. Two charging profiles are run in the models and compared: home charging and work charging. Home charging implies that most electric vehicles are charged in the evenings when people arrive home from work. This charging strategy requires less wind and solar generation capacity, less energy storage capacity but more dispatchable power generation. In contrast, having work charging EVs requires more VRE capacity, especially solar capacity, because the cars are charged during the day when solar generation is at a maximum. It also requires more storage energy capacity but less dispatchable generation.

The last variable introduced in the models is curtailment. Ideally, curtailed energy should be zero because solar and wind energy are free and should not be wasted. However, a case with a 10% of energy curtailment was simulated, and the results show that the dispatchable generation capacity increases but the storage energy capability significantly decreases, which could be beneficial in practice due to the current high cost of storage technologies.

9.2 Recommendations for Future Work

Based on the extensive number of model runs and sensitivity analysis cases carried out on this work, several recommendations can be made to improve the future models.

For this work, wind and solar hourly capacity factor profiles were available for one year. However, it is possible to estimate more years of wind and solar production based on weather data and run the optimization models for more than one year. This will give more results, and the worst or average case can be chosen as the final solution.

If the power system is geographically larger, it would be important to optimize the location of wind and solar plants or what it is called spatial optimization. This would require having the wind and solar production data profiles for all the selected locations.

Regarding the optimization model for storage and generator, it is possible to add more constraints that can better represent the hour by hour operation of the generation resources, especially if the technology to be used is known in advanced. For example, if the dispatchable generator to be used is biomass, the minimum generation level, ramp rates and minimum downtimes can be included in the optimization model to improve the results. However, this changes the linear programming model to mixed integer linear programming model that requires more computer power and advanced optimization solvers.

To avoid stability issues in the operation of the power system, a dispatchable generator may have to run all year round at a certain minimum level of output power. This is because the rotational unit can provide inertia to the system. If this is the case, a new case study can be easily run in the model including this constraint in the formulation. Another important measure necessary to ensure stability is the spinning reserves. The model can include the operating reserves as a constraint in the formulation as well.

To obtain more specific results using this methodology, Barbados should clarify some of the unknown variables in the system so that they can be included in the model as inputs. For example, if Barbados knows the amount of wind capacity to be installed, the technology and the corresponding production profiles, the results for solar and the other generation resources can be better estimated.

Finally, different technology costs can be input into the cost optimization models to see the effects of cost variation, especially for the model that optimizes storage and dispatchable generation.

References

- [1] National Renewable Energy Laboratory, “Energy Snapshot - Barbados,” 2015.
- [2] Barbados Today, “A 3\$ billion exercise: Converting to 100% renewable nergy costly,” *Barb. Today Newsp.*, pp. 12–13, Jul. 2018.
- [3] IRENA, “Quantitative Analysis for the Barbados Renewable Energy Roadmap,” pp. 1–39, 2016.
- [4] S. Boyd and L. Vandenberghe, *Convex Optimization*. Cambridge: Cambridge University Press, 2004.
- [5] Akala *et al.*, “Determined optimization technique for solving over-determined linear systems,” *Am. J. Phys. Educ*, vol. 5, no. 3, 2011.
- [6] M. Gulliksson, “Algorithms for Overdetermined Systems of Equations,” *Inst. Inf. Process.*, 1993.
- [7] J. A. Cadzow, “Minimum ℓ_1 , ℓ_2 , and ℓ_∞ Norm Approximate Solutions to an Overdetermined System of Linear Equations,” *Digit. Signal Process. A Rev. J.*, vol. 12, no. 4, pp. 524–560, 2002.
- [8] O. Hohmeyer, “A 100 % renewable Barbados and lower energy bills: A plan to change Barbados ’ power supply to 100% renewable and its possible benefits,” Europa-Universität Flensburg Center for Sustainable Energy Systems (CSES), Flensburg, Germany, 2015.
- [9] W. Short and V. Diakov, “Matching Western US electricity consumption with wind and solar resources,” *Wind Energy*, vol. 16, no. 4, pp. 491–500, May 2013.
- [10] W. D. Grossmann, I. Grossmann, and K. W. Steininger, “Distributed solar electricity generation across large geographic areas, Part I: A method to optimize site selection, generation and storage,” *Renew. Sustain. Energy Rev.*, vol. 25, pp. 831–843, Sep. 2013.
- [11] J. Pereira, R. A. Ferreira, J. A. M. Sousa, J. Lagarto, and A. Martins, “Optimizing the renewable generation mix in the Portuguese power system based on temporal and spatial diversity,” *Int. Conf. Eur. Energy Mark. EEM*, pp. 1–5, 2014.
- [12] S. Killinger, K. Mainzer, R. McKenna, N. Kreifels, and W. Fichtner, “A regional optimisation of renewable energy supply from wind and photovoltaics with respect

- to three key energy-political objectives,” *Energy*, vol. 84, pp. 563–574, 2015.
- [13] W. Zappa and M. van den Broek, “Analysing the potential of integrating wind and solar power in Europe using spatial optimisation under various scenarios,” *Renew. Sustain. Energy Rev.*, vol. 94, pp. 1192–1216, May 2018.
- [14] C. T. M. Clack, Y. Xie, and A. E. MacDonald, “Linear programming techniques for developing an optimal electrical system including high-voltage direct-current transmission and storage,” *Int. J. Electr. Power Energy Syst.*, vol. 68, pp. 103–114, Jun. 2015.
- [15] The Barbados Light & Power Company Limited, “2012 Integrated Resource Plan,” 2014.
- [16] AWS Truepower, “Synthesis of wind and solar production data for Barbados,” General Electric, New York, United States, 2014.
- [17] D. R. Cameron and G. R. J. Thatcher, “Mechanisms of Reaction of Sulfate Esters: A Molecular Orbital Study of Associative Sulfuryl Group Transfer, Intramolecular Migration, and Pseudorotation,” *J. Org. Chem.*, vol. 61, no. 17, pp. 5986–5997, Jan. 1996.
- [18] “Average and Record Conditions at Bridgetown, Barbados.” [Online]. Available: http://www.bbc.co.uk/weather/world/city_guides/results.shtml?tt=TT003280. [Accessed: 21-Feb-2019].
- [19] ESMAP, SOLARGIS, WB, and IFC, “Global Solar Atlas,” *Global Solar Atlas*, 2019. [Online]. Available: <https://globalsolaratlas.info/>. [Accessed: 22-Feb-2019].
- [20] “Barbados Weather and Climate,” 2014. [Online]. Available: <https://barbados.org/weather.htm#.XHQMUohKi70>. [Accessed: 25-Feb-2019].
- [21] M. K. Chang, J. D. Eichman, F. Mueller, and S. Samuelsen, “Buffering intermittent renewable power with hydroelectric generation: A case study in California,” *Appl. Energy*, vol. 112, pp. 1–11, 2013.
- [22] P. L. Joskow, “Comparing the cost of intermittent and dispatchable generation technologies,” *Am. Econ. Rev.*, vol. 100, pp. 238–241, 2011.
- [23] “Where Geothermal Energy Is Found - Energy Explained, Your Guide To Understanding Energy - Energy Information Administration,” *U.S. Energy*

- Information Administration*, 2016. [Online]. Available: https://www.eia.gov/energyexplained/index.php?page=geothermal_where. [Accessed: 11-Mar-2019].
- [24] P. K. Alexander Ochs; Mark Konold; Katie Auth; Evan Musolino, “Caribbean Sustainable Energy Roadmap and Strategy,” *Worldwatch Inst.*, p. 106, 2015.
- [25] “Barbados rivers.” [Online]. Available: <https://barbados.org/barbados-rivers.htm#.Xla6gyhKiUk>. [Accessed: 11-Mar-2019].
- [26] “Biomass for Electricity Generation | WBDG - Whole Building Design Guide.” [Online]. Available: <https://www.wbdg.org/resources/biomass-electricity-generation>. [Accessed: 11-Mar-2019].
- [27] “Barbados Sugar cane production, 1961-2018 - knoema.com.” [Online]. Available: <https://knoema.com/atlas/Barbados/topics/Agriculture/Crops-Production-Quantity-tonnes/Sugar-cane-production>. [Accessed: 12-Mar-2019].
- [28] IRENA, *Electricity storage and renewables: Costs and markets to 2030*, no. October. 2017.
- [29] S. P. S. Badwal, S. S. Giddey, C. Munnings, A. I. Bhatt, and A. F. Hollenkamp, “Emerging electrochemical energy conversion and storage technologies,” *Front. Chem.*, vol. 2, p. 79, Sep. 2014.
- [30] B. McNamara and L. Rosenwax, “The mismanagement of dying,” *Heal. Sociol. Rev.*, vol. 16, no. 5, pp. 373–383, Dec. 2007.
- [31] S. Rehman, L. M. Al-Hadhrami, and M. M. Alam, “Pumped hydro energy storage system: A technological review,” *Renewable and Sustainable Energy Reviews*, vol. 44. pp. 586–598, 2015.
- [32] M. Aneke and M. Wang, “Energy storage technologies and real life applications – A state of the art review,” *Applied Energy*, vol. 179. pp. 350–377, 2016.
- [33] A. Akhil *et al.*, “DOE/EPRI 2013 electricity storage handbook in collaboration with NRECA,” *Sandia Rep.*, no. July, p. 340, 2013.
- [34] Lindo Systems Inc., “Lindo Systems Inc.,” in *The Modeling Language And Optimizer*, Lindo Systems Inc., 2018.
- [35] GE Energy, “Western Wind and Solar Integration Study, NREL/SR-550-47434,”

2010.

- [36] General Electric, “Barbados Wind and Solar Integration Study,” 2015.
- [37] ESMAP, SOLARGIS, WB, and IFC, “Global Solar Atlas,” *Global Solar Atlas*, 2019. [Online]. Available: <https://globalsolaratlas.info/?m=sg:ghi>.
- [38] U. S. EIA, “Capital Cost Estimates for Utility Scale Electricity Generating Plants. US Department of Energy, Energy Information Administration,” *US Dep. Energy, Energy Inf. Adm.*, no. November, p. 141, 2016.
- [39] EIA, “U.S. Battery Storage Market Trends,” Washington, DC, 2018.

Appendix A

Wind and solar capacity optimization results for all load demand scenarios

Effect of load demand profile on results in terms of power capacities

Scen.	Load	EV Load	Power (MW)				
			Wind	Solar	Total VRE	Maximum Excess	Maximum Shortage
1	Low	No EV	179.3	106.7	286.0	111.7	-128.2
2	Medium		255.2	151.9	407.1	158.0	-171.0
3	High		344.4	200.4	544.8	211.3	-240.0
4	DSM		151.2	89.4	240.6	94.1	-107.8
5	Low	Home Charging EV	256.9	96.3	353.2	157.5	-228.1
6	Medium		332.8	141.5	474.3	203.9	-271.8
7	High		422.0	190.0	612.0	257.1	-339.0
8	DSM		228.8	79.0	307.8	140.0	-207.9
9	Low	Work Charging EV	204.4	230.8	435.2	136.1	-170.0
10	Medium		280.3	276.0	556.3	170.3	-230.3
11	High		369.5	324.5	694.0	223.5	-260.8
12	DSM		176.4	213.5	389.8	121.9	-155.5

Effect of load demand profile on results in terms of energy capacities

Scen.	Load	EV Load	Annual Energy (MWh/year)					
			Wind	Solar	Total VRE	Excess	Shortage	Total Residual
1	Low	No EV	499,224	187,092	686,316	76,472	-269,156	-192,684
2	Medium		710,580	260,062	970,642	105,783	-375,540	-269,757
3	High		958,969	338,321	1,297,290	144,561	-514,671	-370,110
4	DSM		421,128	159,072	580,200	64,425	-226,725	-162,300
5	Low	Home Charging EV	715,309	170,267	885,576	148,454	-432,231	-283,777
6	Medium		926,665	243,238	1,169,903	174,227	-535,076	-360,849
7	High		1,175,053	321,498	1,496,551	210,711	-671,912	-461,201
8	DSM		637,213	142,249	779,462	137,696	-391,086	-253,390
9	Low	Work Charging EV	569,218	387,470	956,688	85,251	-299,378	-214,127
10	Medium		780,575	460,441	1,241,016	113,640	-404,840	-291,200
11	High		1,028,964	538,699	1,567,663	149,597	-541,149	-391,552
12	DSM		491,121	359,451	850,572	74,747	-258,489	-183,742

Appendix B

Results of residual optimization model, wind and solar capacities, for the three selected scenarios

Scenario 4. DSM load and No EV

Storage MW	Power (MW)					Annual Energy (MWh/year)				
	Wind	Solar	Total VRE	Max. Excess	Max. Shortage	Wind	Solar	Total VRE	Excess	Shortage
0	37.8	63.6	101.4	0.0	-109.0	105,187	117,477	222,664	0	-519,836
20	69.1	63.6	132.7	20.0	-108.5	192,420	117,370	309,790	258	-432,968
40	100.9	60.5	161.4	40.0	-108.2	280,824	112,476	393,300	4,978	-354,177
60	125.6	66.4	192.0	60.0	-108.0	349,848	121,866	471,714	21,937	-292,722
80	143.6	78.3	221.9	80.0	-107.8	399,931	141,104	541,035	46,657	-248,121
100	151.2	89.4	240.6	94.1	-107.8	421,127	159,073	580,200	64,425	-226,725
120	151.2	89.4	240.6	94.1	-107.8	421,127	159,073	580,200	64,425	-226,725
140	151.2	89.4	240.6	94.1	-107.8	421,127	159,073	580,200	64,425	-226,725
160	151.2	89.4	240.6	94.1	-107.8	421,127	159,073	580,200	64,425	-226,725
180	151.2	89.4	240.6	94.1	-107.8	421,127	159,073	580,200	64,425	-226,725
200	151.2	89.4	240.6	94.1	-107.8	421,127	159,073	580,200	64,425	-226,725
220	151.2	89.4	240.6	94.1	-107.8	421,127	159,073	580,200	64,425	-226,725
240	151.2	89.4	240.6	94.1	-107.8	421,127	159,073	580,200	64,425	-226,725
260	151.2	89.4	240.6	94.1	-107.8	421,127	159,073	580,200	64,425	-226,725
280	151.2	89.4	240.6	94.1	-107.8	421,127	159,073	580,200	64,425	-226,725

Scenario 7. High load demand plus home charging electric vehicles load

Storage MW	Power (MW)					Annual Energy (MWh/year)				
	Wind	Solar	Total VRE	Max. Excess	Max. Shortage	Wind	Solar	Total VRE	Excess	Shortage
0	150.2	96.0	246.2	0.0	-342.8	418,177	169,723	587,900	0	-1,369,853
20	175.3	102.1	277.5	20.0	-342.2	488,209	179,640	667,849	132	-1,290,035
40	200.5	107.7	308.1	40.0	-341.6	558,242	188,587	746,829	1,322	-1,212,245
60	225.6	113.0	338.7	60.0	-341.0	628,275	197,233	825,508	5,452	-1,137,697
80	250.8	118.4	369.2	80.0	-340.4	698,307	205,879	904,186	14,161	-1,067,727
100	275.9	123.7	399.7	100.0	-339.8	768,340	214,525	982,865	27,375	-1,002,263
120	301.1	129.1	430.2	120.0	-339.2	838,372	223,171	1,061,543	45,193	-941,402
140	326.2	132.2	458.4	140.0	-339.0	908,405	228,156	1,136,561	66,457	-887,648
160	351.4	132.7	484.1	160.0	-339.0	978,438	229,056	1,207,494	90,332	-840,591
180	376.3	133.3	509.6	180.0	-339.0	1,048,470	229,955	1,278,425	117,182	-796,508
200	391.2	144.9	536.1	200.0	-339.0	1,089,284	248,788	1,338,072	140,148	-759,828
220	402.0	160.7	562.7	220.0	-339.0	1,119,313	274,240	1,393,553	162,843	-727,042
240	412.8	176.5	589.2	240.0	-339.0	1,149,336	299,696	1,449,032	187,773	-696,493
260	422.0	190.0	612.0	257.1	-339.0	1,175,054	321,497	1,496,551	210,711	-671,913
280	422.0	190.0	612.0	257.1	-339.0	1,175,054	321,497	1,496,551	210,711	-671,913

Scenario 11. High load demand plus work charging electric vehicles load

Storage MW	Power (MW)					Annual Energy (MWh/year)				
	Wind	Solar	Total VRE	Max. Excess	Max. Shortage	Wind	Solar	Total VRE	Excess	Shortage
0	161.9	213.5	375.4	0.0	-269.9	450,871	359,415	810,286	0	-1,148,929
20	187.6	220.9	408.5	20.0	-269.3	522,341	371,492	893,833	198	-1,065,579
40	201.8	241.0	442.7	40.0	-267.6	561,808	403,840	965,648	1,187	-994,754
60	222.8	248.7	471.5	60.0	-267.0	620,365	416,273	1,036,638	3,952	-926,528
80	244.4	255.4	499.8	80.0	-266.4	680,600	427,140	1,107,740	9,331	-860,806
100	266.1	262.1	528.2	100.0	-265.9	740,834	438,006	1,178,840	18,654	-799,028
120	287.7	268.8	556.5	120.0	-265.3	801,069	448,873	1,249,942	32,663	-741,936
140	310.9	273.0	583.9	140.0	-265.0	865,700	455,637	1,321,337	51,974	-689,853
160	335.3	274.4	609.7	160.0	-264.9	933,596	457,847	1,391,443	76,158	-643,929
180	346.1	290.2	636.2	180.0	-263.6	963,616	483,305	1,446,921	96,400	-608,693
200	356.9	305.9	662.8	200.0	-262.3	993,760	508,760	1,502,520	119,250	-576,065
220	367.6	321.7	689.3	220.0	-261.0	1,023,670	534,212	1,557,882	144,829	-546,162
240	369.5	324.5	694.0	223.5	-260.8	1,028,963	538,699	1,567,662	149,597	-541,149
260	369.5	324.5	694.0	223.5	-260.8	1,028,963	538,699	1,567,662	149,597	-541,149
280	369.5	324.5	694.0	223.5	-260.8	1,028,963	538,699	1,567,662	149,597	-541,149

Appendix C

LINGO Code

Residual Optimization Model for Wind and Solar:

MODEL:

SETS:

```
HOURL/1..8760/:  
    FactorS1,    !Hourly capacity factors central solar PV %;  
    FactorS2,    !Hourly capacity factors distributed solar PV %;  
    FactorW1,    !Hourly capacity factors for onshore wind %;  
    L;           !Hourly load demand MW;
```

```
CAPACITY/1/:  
    Wind1,       !Optimal wind power capacity MW;  
    Solar1,      !Optimal central solar PV power capacity MW;  
    Solar2,      !Distributed solar PV power capacity MW;  
    SO;          !Input of storage power capacity;
```

ENDSETS

DATA:

```
FactorS1,FactorS2,FactorW1,L= @OLE ('C:\ \Model2.xlsx'); !Inputs;
```

```
@OLE ('C:\ \Model2.xlsx') = Wind1,Solar1,Solar2,SO; !Outputs;
```

```
SO = ?;
```

ENDDATA

```
!Objective Function;
```

```
MIN = @SUM(HOURL(t): (Wind1(1)*FactorW1(t)+ Solar1(1)*FactorS1(t) +  
Solar2(1)*FactorS2(t) - L(t))^2);
```

```
!Hourly limit on residual power excess;
```

```
@FOR(HOURL(t): Wind1(1)*FactorW1(t)+ Solar1(1)*FactorS1(t) +  
Solar2(1)*FactorS2(t) - L(t)<= SO(1));
```

```
!Power capacity limits;
```

```
Solar2(1) = 50;
```

```
Solar1(1) >= 0;
```

```
Wind1(1) >= 0;
```

END

Cost Optimization Model for Wind and Solar:

MODEL:

SETS:

```
HOURL/1..8760/:  
    FactorS1,    !Hourly capacity factors central solar PV %;  
    FactorS2,    !Hourly capacity factors distributed solar PV %;  
    FactorW1,    !Hourly capacity factors for onshore wind %;  
    L;           !Hourly load demand MW;
```

```
CAPACITY/1/:  
    Wind1,       !Optimal wind power capacity MW;  
    Solar1,      !Optimal central solar PV power capacity MW;  
    Solar2,      !Distributed solar PV power capacity MW;  
    SO;         !Input of storage power capacity;
```

ENDSETS

DATA:

```
FactorS1,FactorS2,FactorW1,L= @OLE ('C:\ \Model2.xlsx'); !Inputs;
```

```
@OLE ('C:\ \Model2.xlsx') = Wind1,Solar1,Solar2,SO; !Outputs;
```

```
SO = ?;  
RPL = 0.9;
```

ENDDATA

```
!Objective Function;
```

```
MIN = 2.05*Solar1(1) + 2.5*Wind1(1);
```

```
!Hourly limit on residual power excess;
```

```
@FOR(HOURL(t): Wind1(1)*FactorW1(t)+ Solar1(1)*FactorS1(t) +  
Solar2(1)*FactorS2(t) - L(t)<= SO(1));
```

```
!Annual energy penetration;
```

```
@SUM(HOURL(t):FactorW1(t))*Wind1(1) +  
@SUM(HOURL(t):FactorS1(t))*Solar1(1)+  
@SUM(HOURL(t):FactorS2(t))*Solar2(1) > = RPL*@SUM(HOURL(t): L(t));
```

```
!Power capacity limits;
```

```
Solar2(1) = 50;  
Solar1(1) >= 0;  
Wind1(1) >= 0;
```

END

Cost Optimization Model for Generator and Storage:

MODEL:

SETS:

```
HOURL/1..8760/:      G,  !Hourly generator power dispatch MW;
                    SD,  !Hourly storage power discharge MW;
                    SC,  !Hourly storage power charge MW;
                    CU,  !Hourly curtailed power MW;
                    H,   !Hourly SOC of storage MWh;
                    RE,  !Hourly residual power excess MW;
                    RS;  !Hourly residual power shortage MW;
```

CAPACITY/1/:

```
GO, !Optimal generator installed power capacity MW;
HO, !Optimal storage energy capacity MWh;
SO, !Input storage power capacity MW;
FHinitial; !Initial state of charge of storage;
```

ENDSETS

DATA:

```
RE,RS = @OLE ('C:\ \Model2.xlsx'); ! Inputs;
```

```
@OLE ('C:\ \Model2.xlsx') = GO,SO,HO,G,CU,H,SC,SD,FHinitial; ! Outputs;
```

```
Gmin = 0;           !Minimum generator power capacity MW;
Gmax = 400;         !Maximum generator power capacity MW;
FHmin = 0;         !Minimum state of charge allowed %;
FHmax = 1;         !Maximum state of charge allowed %;
FHinitial = 0.5;   !Initial state of charge of storage;
Hmin = 0;          !Minimum storage energy capability MWh;
Hmax = 40000;      !Maximum storage energy capability MWh;
CUmaxE = 0;        !Maximum annual curtailed energy %;
SO = ?;            !Input storage power capacity MW;
COSTGCAP = 4985000; !Capital cost of generator $/MW;
COSTHCAP = 650000; !Capital cost of energy storage capability $/MWh;
COSTGOPE = 4.2;    !Operational cost of generator $/MWh;
COSTSOPE = 8;      !Operational cost of storage $/MWh;
```

ENDDATA

! Objective function;

```
[OBJ] MIN = COSTGCAP*@SUM(CAPACITY: GO(1))+ COSTHCAP*@SUM(CAPACITY:
HO(1)) + COSTGOPE*@SUM(HOURL(t):G(t)) + COSTSOPE*@SUM(HOURL(t):SD(t)) +
COSTSOPE*@SUM(HOURL(t):SC(t));
```

!Energy balance constraint;

```
@FOR(HOURL(t): G(t) + SD(t) - SC(t) - CU(t) - RS(t) + RE(t)= 0);
```

!Generator constraints;

```
@SUM(HOURL(t): G(t)) >= @SUM(HOURL(t):RS(t)) - @SUM(HOURL(t):RE(t)) +
@SUM(HOURL(t):CU(t));
@FOR(HOURL(t): G(t) <= GO(1));
```

```

@FOR(HOUR(t): G(t) >= Gmin);
GO(1) >= Gmin;
GO(1) <= Gmax;

!Curtailement constraints;
@FOR(HOUR(t): CU(t) >= 0);
@FOR(HOUR(t): CU(t) <= SO(1));
@SUM(HOUR(t): CU(t)) = CUmxE*@SUM(HOUR(t):RE(t));

!Storage Energy constraints;
@FOR(HOUR(t)| t #GT# 1: H(t) = H(t-1) + SC(t) - SD(t));
H(1) = FHinitial(1)*HO(1) + SC(1) - SD(1);
@FOR(HOUR(t): H(t) >= FHmin*HO(1));
@FOR(HOUR(t): H(t) <= FHmax*HO(1));
HO(1) >= Hmin;
HO(1) <= Hmax;

!Storage Power Constraints;
@FOR(HOUR(t): SC(t) >= 0);
@FOR(HOUR(t): SD(t) >= 0);
@FOR(HOUR(t): SC(t) <= SO(1));
@FOR(HOUR(t): SD(t) <= SO(1));
@FOR(HOUR(t): SD(t) - RS(t) <= 0);
@SUM(HOUR(t): SC(t)) >= @SUM(HOUR(t):RE(t)) - @SUM(HOUR(t):CU(t));
@SUM(HOUR(t): SD(t)) >= @SUM(HOUR(t):RE(t)) - @SUM(HOUR(t):CU(t));

END

```

Curriculum Vitae

Candidate's full name: Franco Esteban Perez Sanchez

Universities attended:

Universidad de Santiago de Chile, 2008-2014, Bachelor's Degree of Electrical Engineering

University of Windsor, Winter 2013, Exchange Student Electrical Engineering

Undergraduate Thesis:

Ground fault neutralizers for the medium voltage distribution system of local utility, 2014